4-16-2010

Comparison and Improvement of Different Access Methods in Femtocell Networks

İbrahim Demirdögen
University of South Florida

Comparison and Improvement of Different Access Methods in Femtocell Networks

by

İbrahim Demirdöğen

A thesis submitted in partial fulfillment
of the requirements for the degree of
Master of Science in Electrical Engineering
Department of Electrical Engineering
College of Engineering
University of South Florida

Major Professor: Hüseyin Arslan, Ph.D.
Paris Wiley, Ph.D.
Wilfrido Moreno, Ph.D.

Date of Approval:
April 16, 2010

Keywords: Femtocell, Open Access, Closed Access, Closed Subscriber Group

DEDICATION

To my Parents,

My Mom and My Dad,

Fatma Demirdöğen and Hasan Hüseyin Demirdöğen

ACKNOWLEDGEMENTS

First, I would like to thank my advisor Dr. Hüseyin Arslan for his guidance, encouragement, and continuous support throughout my M.Sc. studies. It has been a privilege to have the opportunity to do research as a member of Dr. Arslan's research group. I wish to thank Dr. Paris Wiley, and Dr.Wilfrido Moreno for serving in my committee and for offering their valuable feedback. I hope to be able to benefit from their profound knowledge and experience in the future, as well.

I am grateful to Dr. Ismail Güvenç not only for advising me throughout our collaboration with NTT DOCOMO, but also for his sincere friendship. I also want to acknowledge Dr. Mustafa Emin Şahin from DOCOMO USA Labs for his support and sincere friendship and support throughout my experience in USF.

I owe much to my friends Hasan Basri Çelebi, Sabih Güzelgöz, Özgür Yürür, Evren Terzi, Dr. Hisham Mahmoud, Ali Görçin, Ismail Bütün, Murad Khalid, M. Bahadır Çelebi, Alphan Şahin, Dr. Bilal Babayiğit, Dr. Serhan Yarkan, M. Cenk Ertürk, Hazar Akı, and Sadia Ahmed. We shared so many things with them over the years that we spent together. They also taught me so many virtues. Sincere friendship to start with, unselfishness, tolerance, and helpfulness. I am grateful to them for making me a better person.

I also want to express my gratitude to my friends in the Turkish community in Tampa, FL, especially to Ismail Ulukaya, Ömer Özbek, Selman Türk, Fatih Demir, Erdem Önsal, Salih Erdem, and Erdoğan Bulut for their support to us, students, whenever we need it.

My sincere appreciation goes to my dear brothers Oğuz, and Yavuz and my dear sister Sümeyya for leading me to the right direction, and always encouraging me for pursuing higher degrees. It is not possible to thank them enough, but I want them to know that I will be grateful to them throughout my life.

TABLE OF CONTENTS

LIST OF TABLES

LIST OF FIGURES

COMPARISON AND IMPROVEMENT OF DIFFERENT ACCESS METHODS IN FEMTOCELL NETWORKS

İbrahim Demirdöğen

ABSTRACT

A variety of wide band wireless systems have been pushed towards their limits in order to meet growing interest for high data rate in wireless communications.In particular, the limit due to the spectrum scarcity forces communication systems to utilize the spectrum resource at maximum efficiency level. One of the methods that allow effective spectrum employing is to cover multiple systems over same spectrum source by allowing bearable interference to occur between them. Femtocells have been recently introduced as a remedy to spectrum scarcity and coverage problems in current cellular structures. Femtocells are personal use base stations and they share the spectrum in a way that they can coexist with the macrocell. This thesis provides a critical reviews of different access methods in femtocell networks and further introduces improvements related to these access methods. Simulation results validate capacity improvement of proposed techniques compared to the existing access methods.

CHAPTER 1

INTRODUCTION

Femtocells, low power base stations, are designed to extend mobile operators' coverage area and improve their capacity. They are targeted to operate in cellular licensed band. Femtocells are aimed at being positioned in individual homes and offices and connected to cellular operator's network via digital subscriber line (DSL) or fiber optic cable. They enable mobile operators to move from conventional single-macro base station with high number of users into small coverage area with limited number of users [1].

1.1 Benefits of Femtocell Networks

There are several prominent benefits of femtocells that need to be mentioned [2, 3]:

- Femtocells provide better indoor coverage than macro cells such that more macro base station deployment would be required to reach similar levels of indoor coverage.
- A small number of users is registered to a femtocell with a limited coverage area (e.g. office or home). Therefore, they are capable of providing broadband data and voice services to their users via considerably high bandwidth. This allows operators to pursue new opportunities such as enhancing the quality of voice services provided in cellular networks to a level where it can be comparable to land-line for home and office environments. Thus, eventually, femtocell deployment can be presented as an effective technology replacement for land-line network. Off-load gain that macro cellular network acquires due to the femtocell deployment is also a strong motivation for operators because it allows them to save their costs to provide similar service quality. Ever increasing data demand in mobile broadband data usage forces mobile

operators to continually improve their network capacity. Deployment of femtocells is also expected to be a remedy to this problem by shifting some of the backhaul data traffic from mobile radio access network to broadband wired networks in a significantly less expensive manner.

- It is also a good opportunity for mobile operators to make a distinction in the market by initiating their distinctive functional applications such as intelligent home-office applications where the service provider needs to achieve seamless communication of user handset with other multimedia devices by sensing the mobile handset presence. Immense customer demand can be established by exploiting these potentials based upon how well mobile operators can accomplish the link between mobile handsets

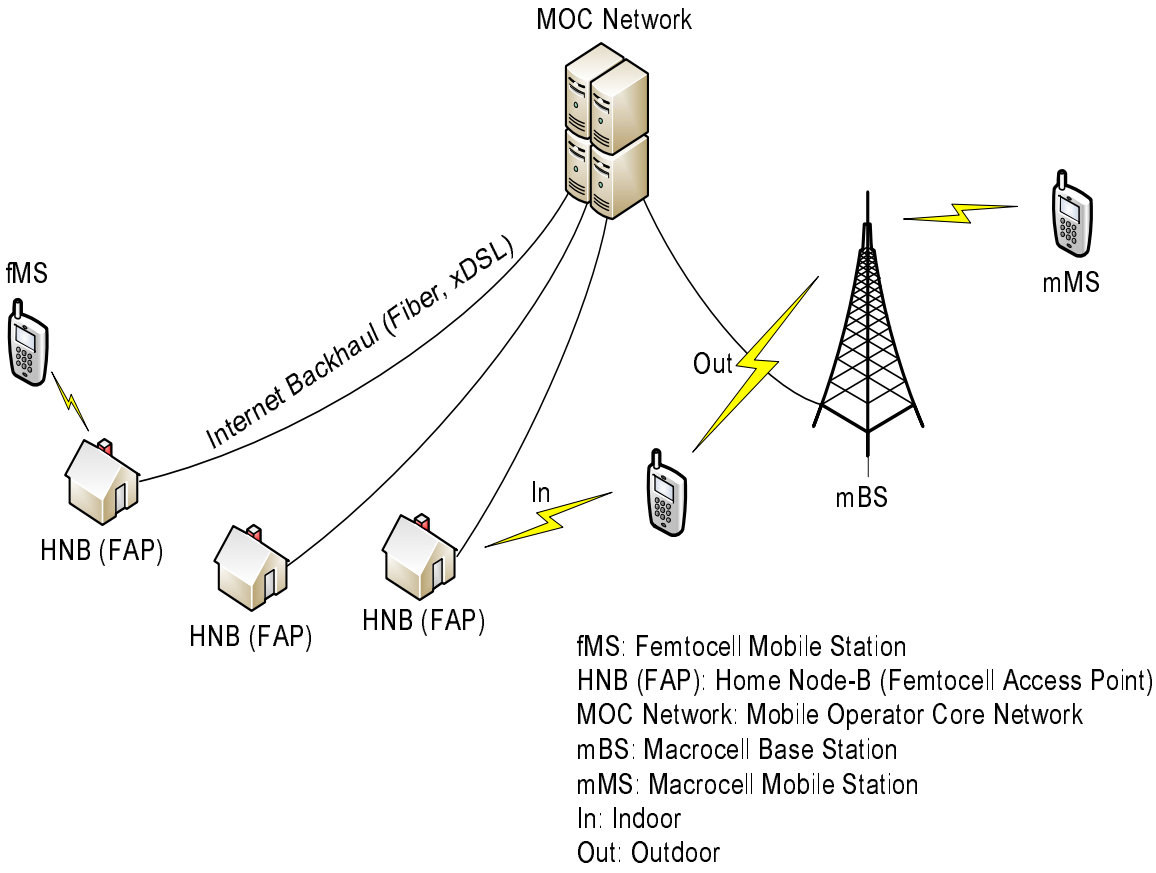

Figure 1.1 Flat architecture of femtocell networks.

with the rest of the network at office or home and how well they can convey the new converged services.

Architecture of femtocell networks, flat network architecture instead of hierarchical type, reduces the number of components to set up a network. Flat network also simplifies the deployment process by eliminating the base station, radio network controller, and complex hierarchical base station relationship that characterize traditional macro access networks [4]. Fig. 1.1 illustrates the flat hierarchical structure of a simple femtocell network. Home Node-Bs (HNBs) are directly connected to the mobile operator core network (MOCN) via internet backhaul (e.g. cable (fiber), xDSL) and the other leg of the MOCN is connected to macrocell network. Thus, it converts packet data nodes of macro-cellular radio network into a small femtocell access points and enables an easy plug-and-play process.

It can be said that based on the advantages and opportunities listed above, femtocells have been one of the open research and development areas in wireless networks for several years.

1.2 Femtocell Challenges

As it happens to every new emerging technology, femtocell concept also has its own technical issues to be addressed and problems to be solved. Some of these problems are listed below with a short explanation: [2, 3]

- Physical and medium access layers related issues : These issues are much more related with power adaptation and frequency assignment of femtocells.
  - Mitigation and management of radio interference : Macrocell to femtocell and femtocell to femtocell interferences should be considered. For the former, femtocells should be aware of the macrocell radio frequency concentration so that they can adjust their environment dependent parameters. In the latter case, when new femtocells are deployed, especially in urban and highly dense suburban environment, existing femtocells should adjust their transmission power accordingly in order to keep the interference level under control.

  - Access control mechanism along with system selection: User handset should be capable of selecting the proper operating network so that corresponding pricing can be employed. Hand off issues among the femtocell networks can also be considered in the scope of cell selection.
  - Frequency resource plan : Keeping the interference level under control is one of the major issues in femtocell deployment. Hence, frequency resource plan is imperative for on managing the interference.

- Network related issues :
  - Scalability and security issues.
  - End-user installation, management and auto-configuration, plug-and-play.
  - Network plan and incorporation with main network (backward compatibility).

1.3 Current and Future Market Status

Cellular companies have been quite interested in femtocell concept because it meets the indoor users data requirements while saving on infrastructure expenses. Nine commercial launches have been achieved in seven different countries until the first quarter of 2010 which are shown in Table 1.1[1] with the commercial prizes, the number of users, and supported technologies.

Femtocell deployments, unlike picocell deployment considered for business environment, have been much more focused on end-user deployment. However, service providers still continue to categorize a number of major user sectors for interesting service scenarios for femtocells such as public access, subway and rural environment. Although the coverage of femtocell service deployment is spreading out year by year all around the world, none of the current service providers has launched the forth generation (4G) (WiMAX or Long Term Evaluation (LTE)) femtocell service [5]. However, first tier cellular companies have been declared that it is highly probable that LTE and following high capacity air interfaces will be deployed via femtocells.

[1]Source: Informa Telecoms & Media

Table 1.1 Current femtocell commercial start on by the end of the first quarter of 2010.

Operator (Country)	Price	Capabilities
Optimus (Portugal)	99.99 euro up front, 7.8 euro monthly	Up to 4 3G-users
SFR (France)	99.99 euro up front	Up to 4 3G-users
NTT DOCOMO (Japan)	$10 per month	Up to 4 3G-users
China Unicom (China)	FAP: CYN 1.200, CYN 10 per month	Up to 4 3G-users
AT&T (USA)	$159	Up to 4 3G-users
Vodafone (UK)	Various options	Up to 4 3G-users
Verizone (USA)	$249.99	up to 3 2G 1xRTT-users
StarHub (Singapore)	$32.1 per month	Up to 4 3G-users
Sprint (USA)	$4.99 per month ($10 unlimited call, $20 family plan)	Up to 3 2G-users

The growth of the femtocell market can also be understood through the trials that have been experienced at all regions. Although the number of public announcement of those trials is quite limited and some of those trials are left as closed boxes, the number of the trial declarations has been increased so far. Some of publicly declared global femtocell trials are summarized in Table 1.2[2].

1.3.1 Industrial Vendors

Femtocell market has been moving from early adopter phase to initial market growth phase. The market can be divided five major sectors [5]:

- End to end Solution Providers & System Integrators: 2009 was a good year for solution provider regarding the trials that they experienced and the solutions that they pro-

[2]Source: Informa Telecoms & Media

Table 1.2 Compilation of publicly declared femtocell worldwide trials by the end of the first quarter of 2010.

Cellular Company	Country
China Mobile	China
Cellcom	USA
Chunghwa Telecom	Taiwan
Comcast	USA
FgupZnisTechnopark	Russia
Maxxis	Malaysia
Mobilkom	Austria
Portugal Telecom	Portugal
T-Mobile	Germany, Poland
TDC	Denmark
Telefonica O2	Europe
TIM	Italy
Vodafone	Spain

vided for initial market phase. Currently nine worldwide end-to-end solution providers and femtocell systems integrators are present. The potential of the market is confirmed through the attention of some pioneer companies in this sector such as Alcatel-Lucent, Huawei and Cisco.

- Femtocell Access Point (FAP): Solutions for customer premises equipment (CPE) have been expanding such that a variety of smart algorithms has been proposed in order to get rid of the interference which constitutes major attention of the cellular operators. Today, approximately fifty on hand or announced items are offered to the market by

twenty six femtocell CPE producer. Solutions for integration of broadband access technologies to the CPE can be standalone or integrated. Vendors keep expanding on their product ranges such as including the enterprise and larger area femtocells.

- Femtocell Core Network: The vendors in this section of the femtocell market usually deal with the core network components related to security, provisioning and integration of the femtocell services into the current core network of cellular operators. Approximately nineteen vendors exist in the market for now who are also interested in security gateways, femtocell gateways, convergence servers and management of HNB.

- Component, Tools & Software: Strong femtocell market ecosystem is completed by the component vendors, development and test tool as well as protocol/system software producers. They have an imperative contribution to make the market improvement speedy. Hardware platform producers such as silicon providers also keep developing on the platforms in order to provide a more efficient higher capacity FAPs to the FAP vendors.

These five legs of the market constitute a healthy femtocell ecology and enable rapid penetration of femtocell concept to the end users. The progress in the femtocell market has been accelerating year by year and product range also has been expanding. Flexible reference platforms have been introduced in order to produce FAPs to support broadband access technologies.

1.3.2 Future Expectations

According to some research companies such as "Juniper Research", "ABI Search", and "Informa Telcoms & Media", the market is expected to keep growing exponentially over the next few years e.g. 114 million mobile users will be using the femtocell networks via around 49 million FAPs by end of 2014 based on the publicly announced market progress tracks. Moreover, by wide-spreading the femtocell concept throughout the regions, 90% of the service revenues of the cellular companies will be shifted to the femtocell networks.

CHAPTER 2

SIMULATION ENVIRONMENT

Third Generation Partnership Project (3GPP) Forum has various work groups in order to establish appropriate standardization for the new emerging technologies such as LTE, and LTE-Advanced. There are also work groups who are dealing with heterogeneous networks where femtocell deployment is present. At this point, having a baseline for simulation assumptions and parameters is important in order to define the two-tiered network requirements accordingly. By facilitating the alignment of the simulation results, valuable inferences and comparisons can be obtained. Although the discussions associated with assumptions and parameters are not finalized, a brief summary of key simulation assumptions and parameters of the present agreement is given in Table 2.1 for the macrocell network and in Table 2.2 for the femtocell network based on the discussions in [6].

Besides the Table 2.1 and Table 2.2, in [7] various numbers of femtocells (N) are uniformly distributed within the macrocell where N is 1, 2, 4, or 10 per macrocell coverage area. Also, total number of users (N_{tot}) is set to 60 users for each entire macro area. Femtocell has up to 4 users (N_{f}) and remaining users ($N_{\text{tot}} - (N_{\text{f}}N)$) are uniformly distributed to the macrocell area. Coverage of a femtocell is assumed to be 40 m and the minimum distance between new node and regular nodes is assumed to be larger than 35 m.

Although a variety of different parameters is delivered by the meeting documents, there are also some parameters which are re-defined in almost every document implying that parameters are not settled yet. One of these parameters is path loss model employed for user equipments (UE) because there are variety of scenarios that should be considered such as suburban and urban (dense) deployment with different femtocell node deployments such

Table 2.1 Parameters and assumptions for macrocell system.

Parameter	Assumption
Cellular Layout	Hexagonal grid, 3 sectors per site, reuse 1
Inter-site distance	500 m or 1732 m.
Number sites	19 (=57 cells) or 7 (=21 cells)
Carrier Frequency	2 GHz
Shadowing standard deviation	8 dB
Penetration Loss (Wall Loss)	10dB or 20dB
Number of BS antennas	2 Rx, 2 Tx
Number of UE antennas	2 Rx, 1 Tx
Total BS TX power (P_{tot})	46 dBm
UE distribution	UE distribution UEs distributed with uniform density within the indoors/outdoors macro coverage area.
UE speeds of interest	3 km/h
DL Receiver Type	Maximum ratio combining (MRC) for single stream or Minimum mean square estimation (MMSE) for multiple.
UL Receiver Type	MRC

as dual-stripe, and 5 $\times$ 5 grid model. Path loss model given in [8] is employed in this simulation which explained in detail in Section 2.1.

Table 2.2 Parameters and assumptions for femtocell system.

Parameter	Assumption
Femtocell Frequency Channel	Co-Channel (Same frequency as macrocell) or Dedicated Channel (Adjacent frequency as macrocell)
Number Rx antennas HeNB	2
Exterior wall penetration loss	10 or 20 dB
Shadowing standard deviation	4 dB
Min/Max HeNB Tx power	0/20 dBm

2.1 Simulation Environment Description

As an initial step, simpler methodology is considered to be able to simulate femtocells deployment schemes and observe the effects of them on cellular network. Femtocells are assumed to exist in the center of uniformly distributed single floor buildings within the macrocell area. Simulation parameters are kept as flexible as possible such that the parameters such as inter distance length of the macrocell, size of houses, street width, number of users, building penetration can be changed by using the graphical user interface (GUI) created in MATLAB. Besides power control mechanism is also added as an option.

Fig. 2.1 shows the main GUI which helps to define the scenario to be simulated. Femtocell coverage with/without potential femtocell location and macrocell coverage are seen through the window with a color bar indicating power image (dBm/Hz) of the entire cell. Capacity cumulative distribution function (CDF) of either macrocell or femtocell is also given by this interface as an output of defined scenario. Every CDF has three labels indicating “outdoor user”,“indoor user” and “all users” also median capacities of those user types are given at the bottom of the interface.

Fig. 2.2 shows macrocell base station settings, femtocell base station settings, user equipment settings and channel settings. Main base station parameters such as carrier frequency,

transmission powers, antenna gains, available total transmission bandwidth and femtocell overlapped transmission bandwidth ratio (in case of adjacent channel assignment), scheduling scheme of the bandwidth are defined by using "MNB MUE Settings" interface. For the channel settings part, various channel models are implemented according to [8] along with the wall penetration loss.

2.1.1 Simulation Parameters and Path Loss Models

In this section simulation parameters and path loss models used in simulator are presented. Channel settings which are selected based mostly on [8] consist of three parts:

- Indoor to indoor path loss model : ITU-R P.1238 is considered as path loss between indoor transmitter-receiver couple. Power loss exponent N reflects the combined loss

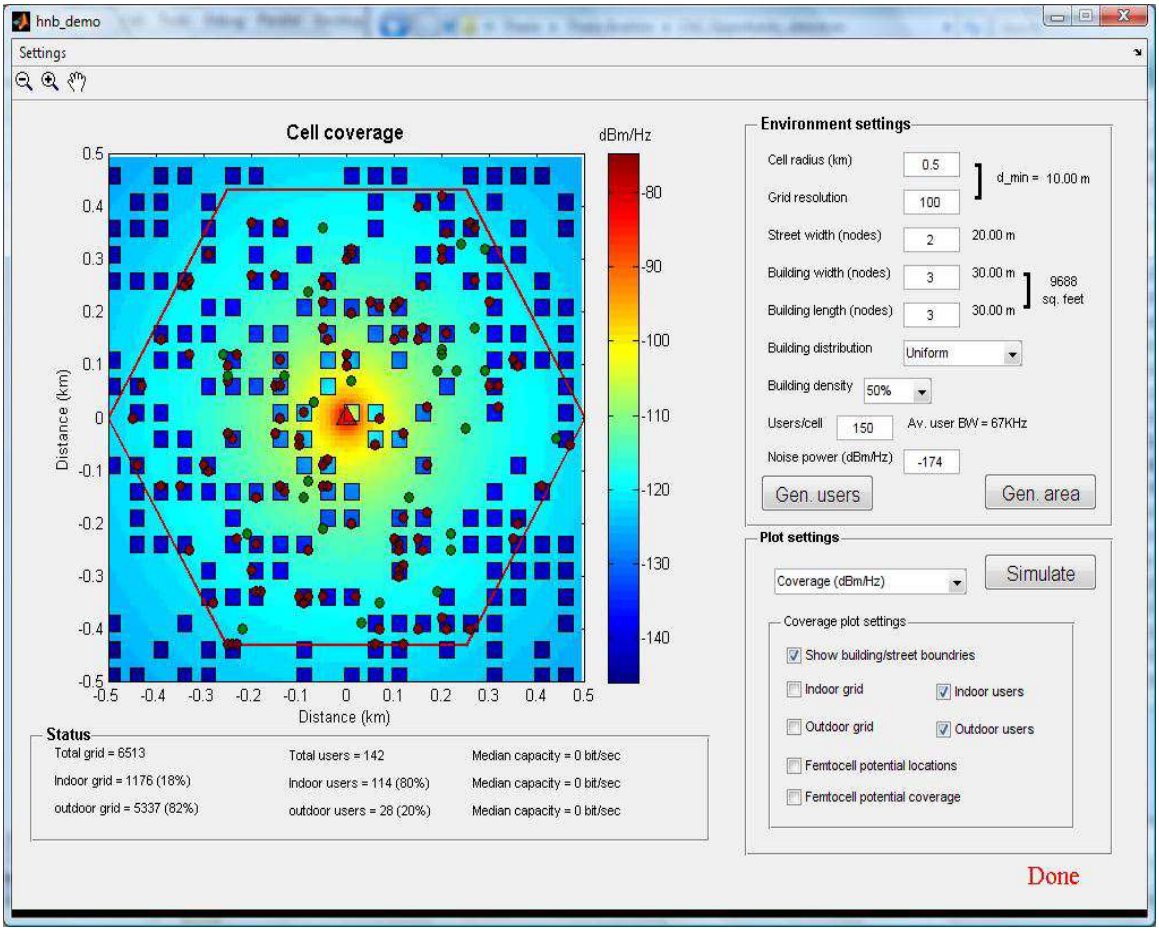

Figure 2.1 Simulator main menu.

due to the objects, walls and doors in living space that directly depends upon building type (e.g office, house, apartment,etc.). Path loss term given as

$$L_{\mathrm{dB}} = 20log_{10}F_{\mathrm{c}} + Nlog_{10}d + L_{\mathrm{f}} - 28, \tag{2.1}$$

where F_{c} is the central transmission frequency in MHz, N distance power loss coefficient, d is the transmitter receiver separation in meter, L_{f} is the floor penetration factor in dB. Note that at least 1 meter distance is necessary in order to calculate the path loss properly. One key advantage of the model is that it does not need any specific information describing the indoor environment such as number of walls and windows between two ends.

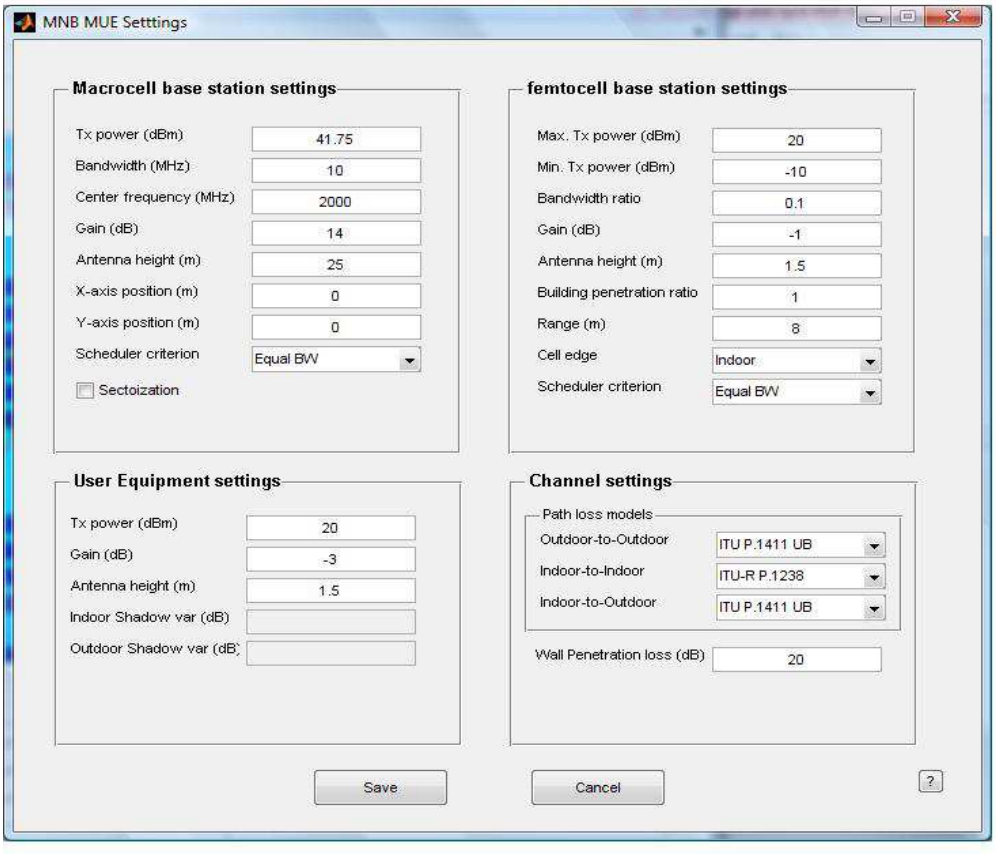

Figure 2.2 MNB and MUE settings.

- Outdoor to outdoor path loss model : Users within the cell are assumed to be near femtocell nodes so ITU P.1411 path loss model is employed. ITU P.1411 path loss model is designed for short distance outdoor systems where not more than 1 km range. It is much more applicable the cases where two ends is enclosed by buildings although they are in line-of-sight(LOS). Model gives lower band and upper band expressions for the path loss calculation where the upper band is given as

$$L_{\mathrm{dB}}^{\mathrm{U}} = L_{\mathrm{bl}} + 20 + 25log_{10}\left(\frac{d}{d_{\mathrm{bp}}}\right) \quad where \quad d \leqslant d_{\mathrm{bp}}$$

$$L_{\mathrm{dB}}^{\mathrm{U}} = L_{\mathrm{bl}} + 20 + 40log_{10}\left(\frac{d}{d_{\mathrm{bp}}}\right) \quad where \quad d > d_{\mathrm{bp}} \ , \tag{2.2}$$

and lower bound given as

$$L_{\mathrm{dB}}^{\mathrm{L}} = L_{\mathrm{bl}} + 20log_{10}\left(\frac{d}{d_{\mathrm{bp}}}\right) \quad where \quad d \leqslant d_{\mathrm{bp}}$$

$$L_{\mathrm{dB}}^{\mathrm{L}} = L_{\mathrm{bl}} + 40log_{10}\left(\frac{d}{d_{\mathrm{bp}}}\right) \quad where \quad d > d_{\mathrm{bp}} \ , \tag{2.3}$$

where d is the distance between two ends in meter, d_{bp} is the distance where varying rate of change in the path loss boosts called break point distance. Break point distance d_{bp} is empirically calculated as

$$d_{\mathrm{bp}} \approxeq \frac{4H_{\mathrm{tx}}H_{\mathrm{rx}}}{\lambda} \tag{2.4}$$

where H_{tx} and H_{tx} are the antenna heights of transmitter and receiver above the street level respectively and λ is the wavelength of the signal calculated by (c/F_{c}) where c is the speed of light. L_{bl} in (2.2) and (2.3) is the basic transmission loss at

the break point which is calculated as

$$L_{\text{bl}} = \left| 20log_{10}\left(\frac{\lambda^2}{8\pi H_{\text{tx}} H_{\text{rx}}}\right)\right| \tag{2.5}$$

- Indoor to outdoor path loss model: Outdoor to outdoor is also employed for indoor to outdoor path loss model by adding the corresponding wall penetration loss.

Besides the path loss model, other parameters that used throughout the simulations are given in Table 2.3 as long as they are not indicated as different value. The parameters which are not covered in the initial phase of the simulator are left as future work.

The coverage image based on the received signal strength (RSS) of the macrocell and femtocell networks shown in Fig. 2.3 and Fig. 2.4 respectively with the color bars in dBm/Hz unit. It can be seen from Fig. 2.3 that indoor users are suffer from severe RSS results in poor capacity for that users. On the other hand, Fig. 2.4 shows that femtocells used in indoor can be used as a remedy for the coverage problem and the capacity problem of the indoor users can be handled by deploying femtocells which result in better RSS. Please note that log-normal shadowing effect is not included neither for macrocell nor femtocells so the signal degradation seems quite smooth. These parameters are considered as further version of the simulator.

A macrocell/femtocell scenario as in Fig. 2.3 and Fig. 2.4 are considered with an mBS located in the center of the cell (shown with a triangle). The buildings (squares) and 150 mobile users (circles) are scattered over a 600×600 grid such a way that 80% of the users are indoor whereas 20% of the users are outdoor [6], within the (hexagonal) borders of the macrocell, where 34% of the area is inside the buildings and 66% of the area is outdoors. Cell selection is based on the SINR metric, where MSs join the femtocell/macrocell that has the best SINR. In all simulations, idle femtocells (with no users) are detected and disabled (i.e., their transmit power are set to zero) to minimize interference.

A 3D plot of the RSS received from macrocell and femtocell users is illustrated in Fig. 2.5[1], which shows that (due to isolation provided by the wall penetration loss)

[1]Areas where femtocells provide higher RSS or SINR are marked in black

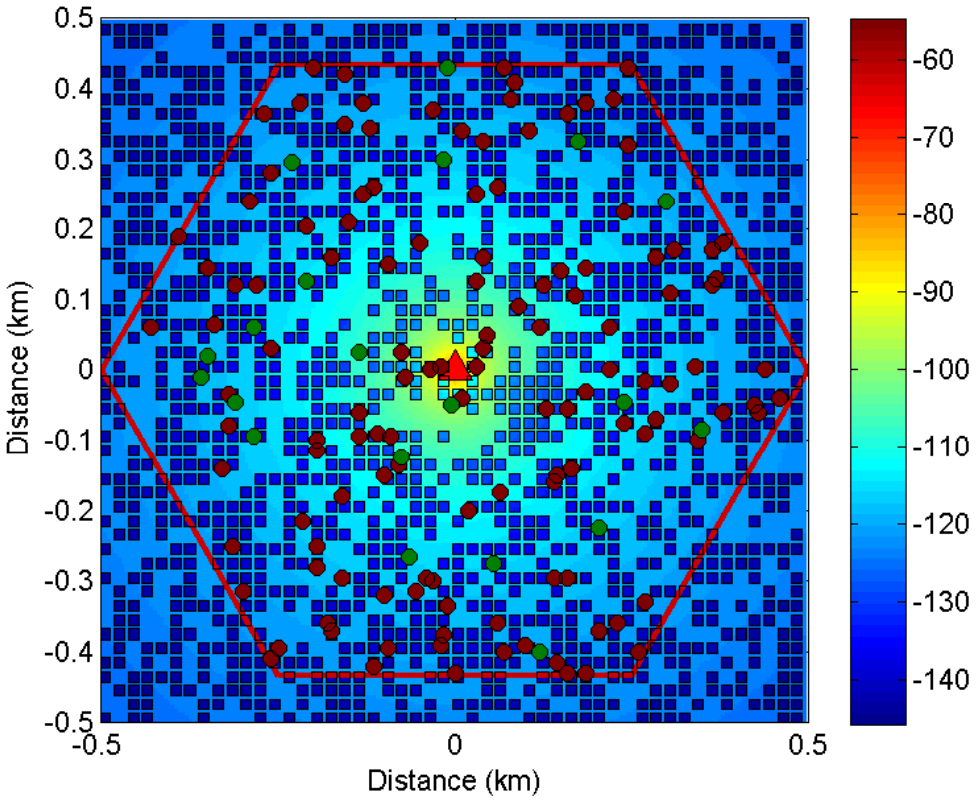

Figure 2.3 Macrocell base station RSS coverage

- RSS from femtocells is significantly larger than RSS from macrocells in indoor locations, resulting in larger capacities with femtocells.
- RSS from femtocells is significantly lower than RSS from macrocells in outdoor locations, typically causing negligible interference from femtocells to macrocell users.

SINR results in Fig. 2.6[2] confirm that there is a sharp drop in the SINR of the macrocell in indoor locations, where femtocells have a good coverage.

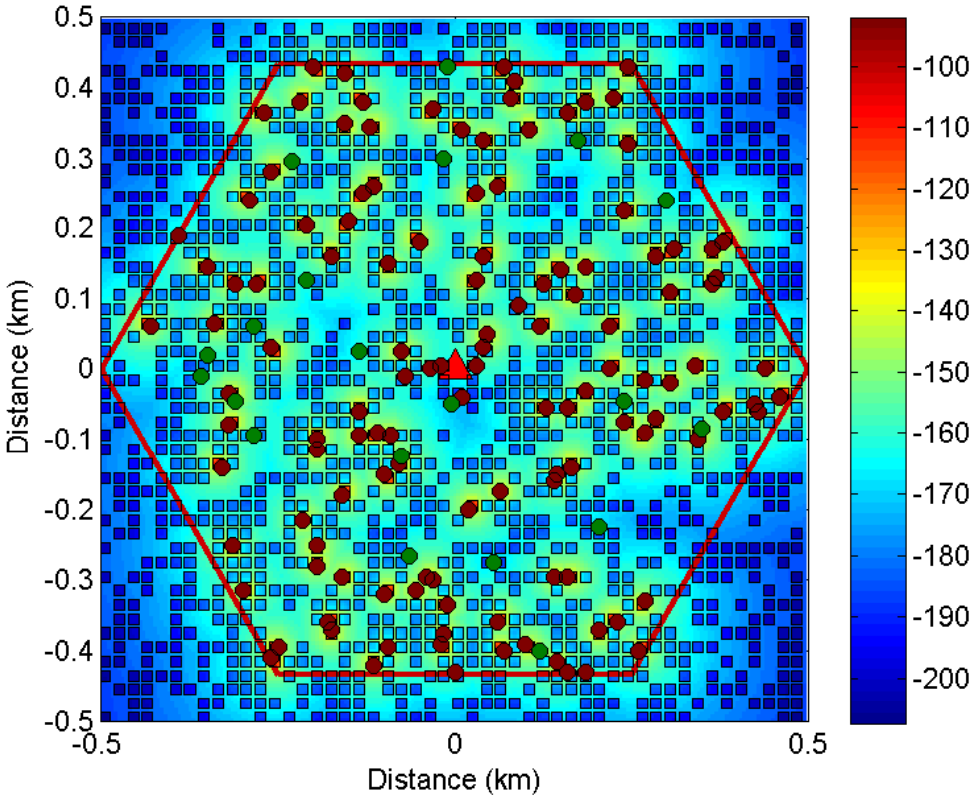

Figure 2.4 Macrocell base station RSS coverage

Table 2.3 Simulation parameters.

Parameter	Value
Central frequency	2.1 GHz
Bandwidth	5 MHz
Coverage (radius) (mBS, fBS)	0.5 km, 8 m
Max. TX power (mBS, fBS)	41.75 dBm, 20 dBm
Thermal noise density	−174 dBm/Hz
Wall penetration loss (WL)	10 dB, 20 dB
Antenna gain (mBS, fBS)	17 dBi, 2 dBi
Feeder/cable loss (mBS, fBS)	3 dB, 1 dB
Antenna heights (mBS, fBS, MS)	15 m, 1.5 m, 1.5 m
House size	15 m ×15 m
Street width	5 m
Distance between grid points	5 m
Number of users per macrocell	150
Indoor area vs. outdoor area	34% vs. 66%
Scheduling strategy	Equal user bandwidth
Indoor/indoor PL model	ITU P.1238
Indoor/outdoor PL model	ITU P.1411 + WL
Outdoor/outdoor PL model	ITU P.1411
Outdoor/indoor PL model	ITU P.1411 + WL

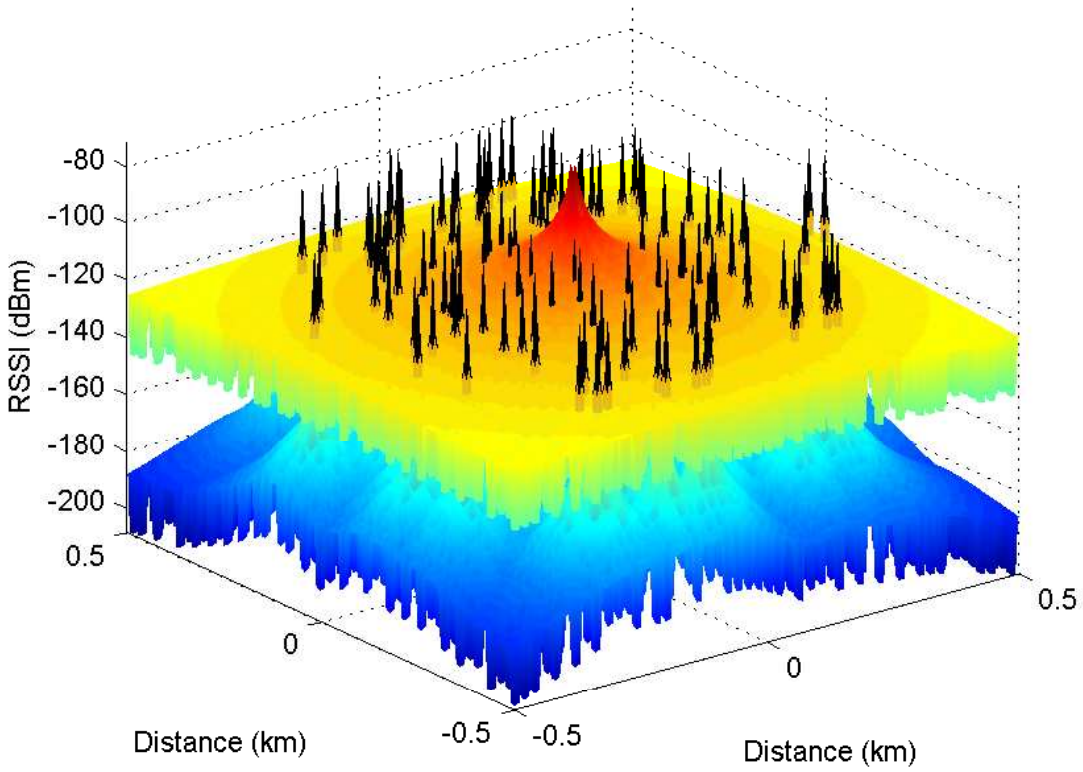

Figure 2.5 RSS of macrocell (top) and femtocell (bottom) base stations.

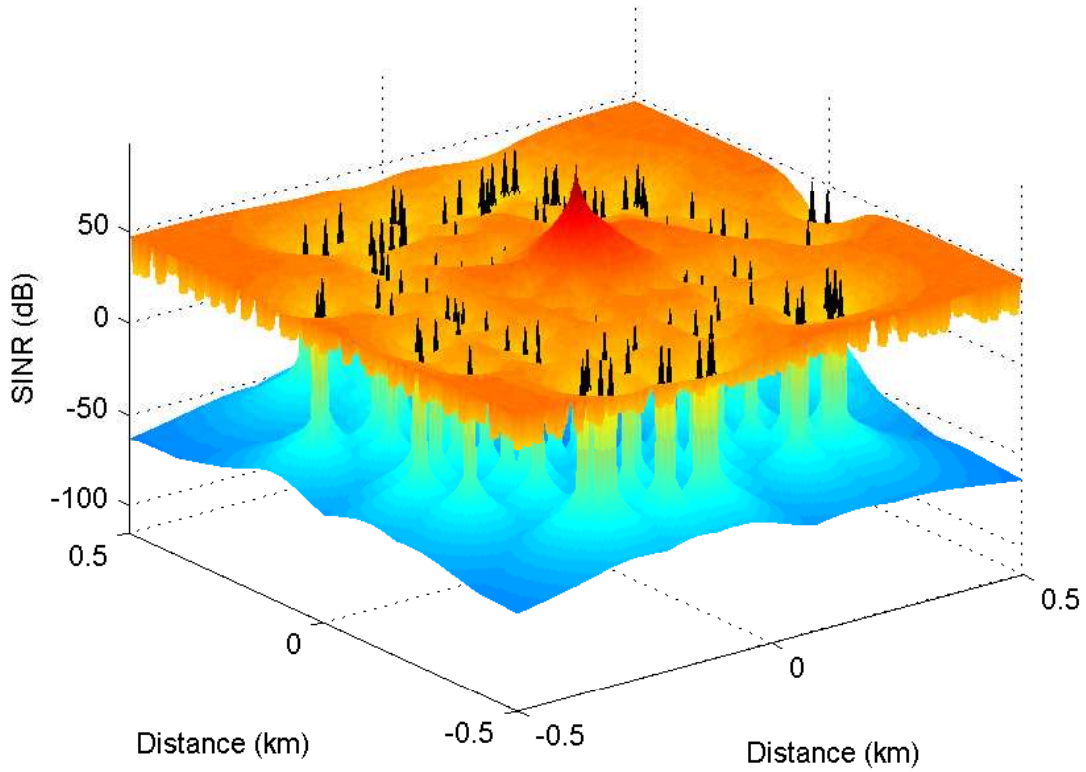

Figure 2.6 SINR of macrocell (top) and femtocell (bottom) base stations..

CHAPTER 3

CLOSED ACCESS FEMTOCELLS

Access configuration of femtocell networks carries critical importance due to the resulting interference scenarios. Especially in closed-access femtocell networks, there might be occur significant interference between the femtocell and the macrocell users. In this chapter, the capacity of closed access femtocell networks employing various dynamic spectrum reuse techniques is evaluated. When there is a macrocell user in the vicinity of a femtocell, the femtocell may dynamically decide not to reuse the spectrum of the macrocell user to avoid interference. We discuss and evaluate the following decision criteria for this purpose: maximum sum capacity, minimum macrocell loss, and minimum effective interference [9]. Computer simulations in realistic settings are provided to demonstrate possible gains with the proposed methods.

Co-channel deployment of femtocell networks with a macrocell network is a popular approach in order to efficiently utilize the available spectrum resources. On the other hand, such co-channel deployments also result in co-channel interference (CCI) problems between the femtocell(s) and the macrocell. In [8, 10], a detailed discussion of six different CCI scenarios between femtocell base stations (fBSs), macrocell base station (mBS), and the mobile stations (MSs) is presented. It is argued that the access control method used by a femtocell may significantly impact the interference scenarios that may be observed by the macrocell and the femtocell users.

There are two major access control options for co-channel femtocell networks. For open access femtocells, any macrocell MS (mMS) is allowed to join a particular femtocell network. This may considerably increase the number of users per femtocell, therefore decreasing the average bandwidth available per femtocell user. Alternatively, for closed access type of

femtocells, the mMSs that may join a particular femtocell are restricted to a certain group. Therefore, a certain femtocell may receive significant interference from (and cause significant interference to) a close-by co-channel mMS, since the mMS will not be granted admission to the femtocell. Example simulation results in [11]- [13] show that open access mode yields better overall system throughput and coverage. On the other hand, compared to closed access mode, open access operation may have several concerns such as privacy issues, extra burden on the backhaul of a femtocell's owner, etc.

In this chapter, we deal with closed access femtocells network where mMSs introduce high interference when they are close to a femtocell. In the literature, [14] proposed a method that mitigates downlink (DL) interference at mMS via spectral resource partitioning and preventing the usage of the overlapped resource at femtocell. In [15], a hybrid spectrum sharing method is proposed which uses an interference threshold for overlapped spectrum avoidance. Cognitively measured interference signature of the network is used by femtocells to determine the reuse priority of channels in [16]. However, detailed evaluations on when to avoid reusing the overlap spectrum at a femtocell is not presented in any of these references. We propose different methods for reuse of the overlap spectrum in a dynamic manner. In particular, three different metrics are considered: maximum sum capacity, minimum mMS loss, and minimum effective interference.

The chapter is organized as follows: Section 3.1 reviews the uplink (UL) and DL capacities of femtocell and macrocell users considering the interference from each other. Section 3.2 proposes and analyzes three different criteria for the reuse of the overlap band (OB) at the femtocells in order to improve the capacity in closed access mode. Simulation results illustrating the potential gains using the proposed methods are presented in Section 3.3 and the last section concludes the chapter.

3.1 Capacities of Macrocell and Femtocell Users

Consider a simple co-channel scenario as illustrated in Fig. 3.1, where there is a femtocell mobile station (fMS) using the spectrum resources of a femtocell, and there is a close-by

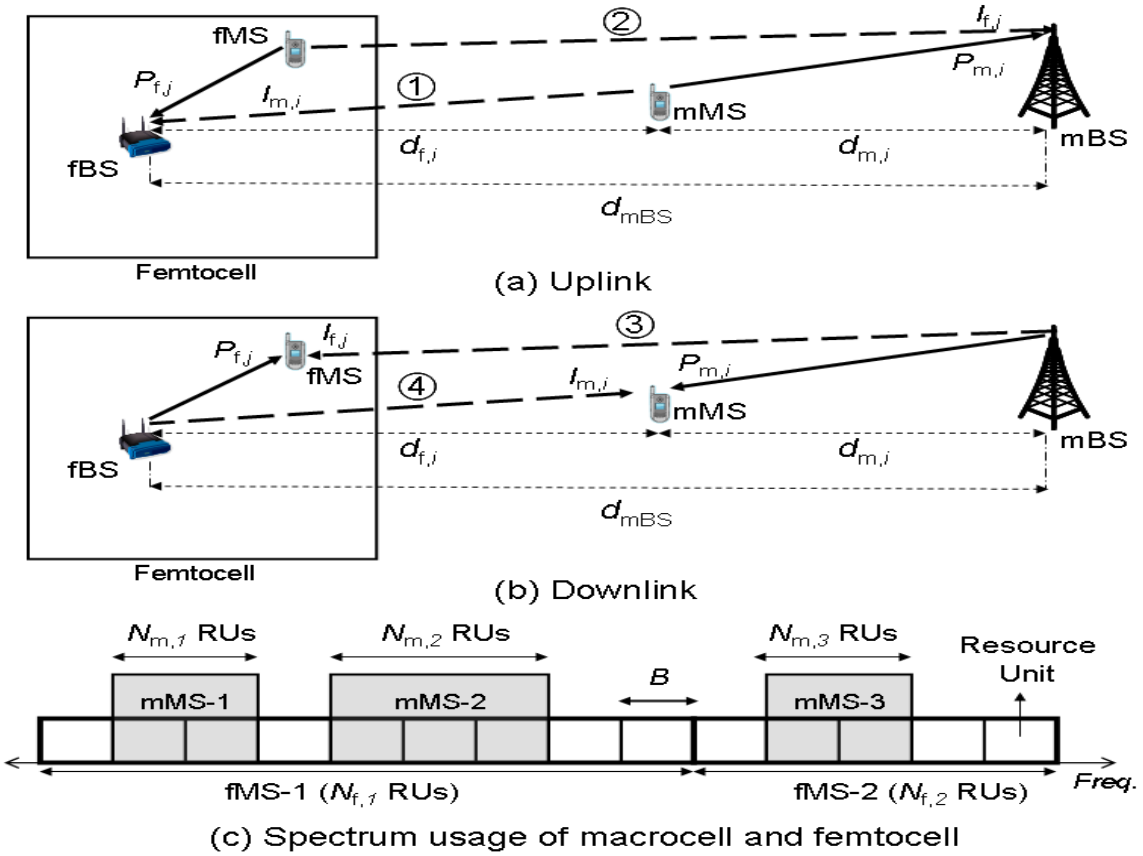

Figure 3.1 System model and interference scenarios for coexisting femtocell and macrocell networks.

mMS within the macrocell space. In such a scenario, there are four different interference scenarios of interest. During the UL, 1) the mMS may interfere to the fBS and 2) the fMS may interfere to mBS, while during the DL 3) the mBS may interfere to the fMS and 4) the fBS may interfere to the mMS[1]. Below, we will first provide capacity formulations for the simple two-user scenario in Fig. 3.1 for the UL and DL, respectively. Since there are typically larger spectrum resources available at a femtocell, it is assumed that the mMS uses only a subset of the resource units (RUs) available to an fMS (see Fig. 3.1(c)). Furthermore, multicarrier transmissions is considered, where each of the RUs can be individually demodulated.

[1]Note that due to synchronization requirements, certain interference configurations such as the uplink interference from the mMS to the downlink reception at an fMS are not possible.

Consider the UL scenario in Fig. 3.1(a), where, as illustrated in Fig. 3.1(c), macrocell and femtocell users utilize overlapping spectrum resources. The distance between an fBS and an associated fMS does not show a large variation due to the small coverage area of a femtocell. On the other hand, depending on the distance $d_{\mathrm{f},i}$ between the fBS and a mMS-i, the femtocell and macrocell users will observe different interference conditions. Then, uplink capacities of the mMS-i and fMS-j can be respectively written as a function of $d_{\mathrm{f},i}$ as

$$C_{\mathrm{m},i}^{\mathrm{UL}}(d_{\mathrm{f},i}) = N_{\mathrm{m},i} B \log\left(1 + \frac{N_{\mathrm{m},i} P_{\mathrm{m},i}}{N_{\mathrm{m},i} I_{\mathrm{f},j} + N_{\mathrm{m},i} B N_0}\right) , \tag{3.1}$$

$$\begin{aligned} C_{\mathrm{f},j}^{\mathrm{UL}}(d_{\mathrm{f},i}) = {} & (N_{\mathrm{f},j} - N_{\mathrm{m},i}) B \log\left(1 + \frac{(N_{\mathrm{f},j} - N_{\mathrm{m},i}) P_{\mathrm{f},j}}{(N_{\mathrm{f},i} - N_{\mathrm{m},i}) B N_0}\right) \\ & + N_{\mathrm{m},i} B \log\left(1 + \frac{N_{\mathrm{m},i} P_{\mathrm{f},j}}{N_{\mathrm{m},i} I_{\mathrm{m},i} + N_{\mathrm{m},i} B N_0}\right) , \end{aligned} \tag{3.2}$$

where i is the mMS index, j is the fMS index, $N_{\mathrm{m},i}$ is the number of resource units used by the mMS-i, $N_{\mathrm{f},j}$ is the number of resource units used by fMS-j, B is the bandwidth per resource unit, $P_{\mathrm{m},i}$ is the received energy for the desired signal at mMS-i, $P_{\mathrm{f},j}$ is the received energy for the desired signal at fMS-j, $I_{\mathrm{m},i}$ is the received energy for the interference signal from mMS-i, $I_{\mathrm{f,j}}$ is the received energy for the interference signal from fMS-j (all of the desired/interference signal energies are per resource unit and interference terms are assumed to have a Gaussian distribution), and N_0 is the noise power. Then, the uplink sum-capacity for the mMS and fMS users can be expressed as[2]

$$C_{\mathrm{tot}}^{\mathrm{UL}}(d_{\mathrm{f},i}) = \sum_{i \in \mathcal{S}_{\mathrm{m}}} C_{\mathrm{m},i}^{\mathrm{UL}}(d_{\mathrm{f},i}) + \sum_{j \in \mathcal{S}_{\mathrm{f}}} C_{\mathrm{f},j}^{\mathrm{UL}}(d_{\mathrm{f},i}) , \tag{3.3}$$

where, $\mathcal{S}_{\mathrm{m}}$ is the set of all mMSs of interest and $\mathcal{S}_{\mathrm{f}}$ is the set of all fMSs of interest.

As an alternative to having a co-channel operation, the femtocell may also avoid using the spectrum resources of the mMSs, in order to prevent interference problems. Then, the

[2]While a single interferer is considered in (3.1) and (3.2), this can be easily generalized to multiple interferers. Same remark applies to (3.6).

uplink capacities for the mMS-i and fMS-j can be respectively written as

$$\tilde{C}^{\mathrm{UL}}_{\mathrm{m},i}(d_{\mathrm{f},i}) = N_{\mathrm{m},i} B \log\left(1 + \frac{N_{\mathrm{m,i}} P_{\mathrm{m},i}}{N_{\mathrm{m},i} B N_0}\right) , \tag{3.4}$$

$$\tilde{C}^{\mathrm{UL}}_{\mathrm{f},j}(d_{\mathrm{f},i}) = (N_{\mathrm{f},j} - N_{\mathrm{m},i}) B \log\left(1 + \frac{(N_{\mathrm{f},j} - N_{\mathrm{m},i}) P_{\mathrm{f},j}}{(N_{\mathrm{f},j} - N_{\mathrm{m},i}) B N_0}\right) , \tag{3.5}$$

where, the UL sum-capacity can be expressed as

$$\tilde{C}^{\mathrm{UL}}_{\mathrm{tot}}(d_{\mathrm{f},i}) = \sum_{i \in \mathcal{S}_{\mathrm{m}}} \tilde{C}^{\mathrm{UL}}_{\mathrm{m},i}(d_{\mathrm{f},i}) + \sum_{j \in \mathcal{S}_{\mathrm{f}}} \tilde{C}^{\mathrm{UL}}_{\mathrm{f},j}(d_{\mathrm{f},i}) \ . \tag{3.6}$$

Comparing (3.6) with (3.3), the femtocell no longer benefits from releasing the overlapped bandwidth (OB) in (3.6). However, for smaller mMS-fBS distance $d_{\mathrm{f},i}$, interference in the OB will be significant for both the femtocell and the macrocell as expressed in (3.1) and (3.2). Therefore, avoiding the reuse of the OB as in (3.4) and (3.5) is expected to improve the sum-capacity in (3.6) when there is (are) mMS(s) in the vicinity of femtocell(s). Using a similar approach as the one in above, DL capacity equations with and without reuse of the OB can be easily formulated.

3.2 Closed Access with Dynamic Spectrum Reuse

As discussed in the previous section, even if the mMSs are within the coverage area of a femtocell, they will not be allowed to make a hand-off to the femtocell for the closed access mode. This implies intolerable interference conditions between the mMS and the femtocell. Analysis of $I_{\mathrm{f}}^{\mathrm{diff}}$ which is the ratio of dominant interference to the remaining interferences observed by macrocell user subjected to closed-access mode is given in Fig. 3.2. It can be assumed that the interference observed by CSG macro user is originated from a single femtocell since CSG macro users locate at the right side of the zero.

We consider that the femtocell is capable of implementing perfect spectrum sensing (SS) and uses a dynamic spectrum reuse (DSR) policy in order to benefit from the OB with the mMSs whenever possible. For simplicity, we consider that there is a single significant mMS interferer for a given femtocell. Different criteria may be considered for deciding whether

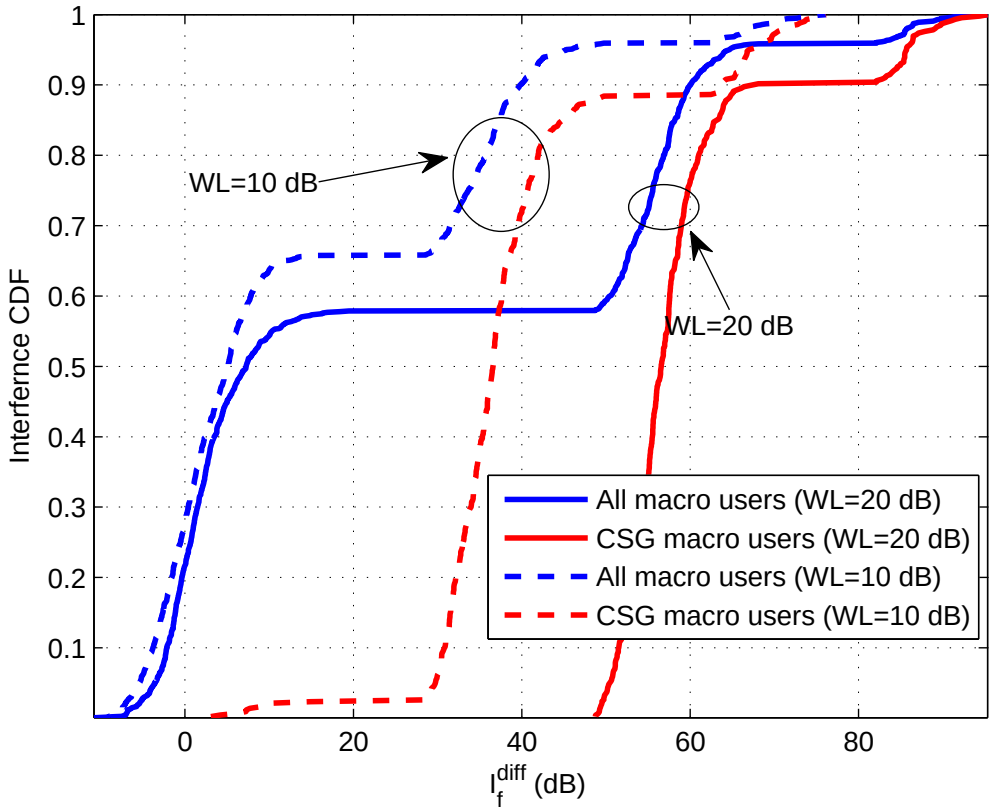

Figure 3.2 Interference analysis of macrocell users subjected to closed access policy.

to use the OB or not at the femtocells. We consider following three criteria for DSR: 1) Maximum sum capacity (MSC), 2) Minimum macrocell loss (MML), and 3) Minimum effective interference (MEI).

3.2.1 Maximum Sum Capacity

One possible criteria for DSR at a femtocell is to maintain a MSC of the femtocell and macrocell users regardless of the distance between the mMS and the femtocell. Then, based on (3.3) and (3.6), the total capacity of all the users of interest can be written as

$$C_{\text{msc}}^{\text{UL}}(d_{\text{f},i}) = \max\left\{C_{\text{tot}}^{\text{UL}}(d_{\text{f},i}), \tilde{C}_{\text{tot}}^{\text{UL}}(d_{\text{f},i})\right\}. \tag{3.7}$$

It can easily be shown that both $\tilde{C}_{\text{tot}}^{\text{UL}}(d_{\text{f},i})$ and $C_{\text{tot}}^{\text{UL}}(d_{\text{f},i})$ are increasing functions of $d_{\text{f},i}$. On the other hand, due to interference conditions, $C_{\text{tot}}^{\text{UL}}(d_{\text{f},i})$ improves at a faster rate compared to $\tilde{C}_{\text{tot}}^{\text{UL}}(d_{\text{f},i})$ and they intersect at a single point. Therefore, in order to obtain the MSC, it is sufficient to find the intersection points of $\tilde{C}_{\text{tot}}^{\text{UL}}(d_{\text{f},i})$ and $C_{\text{tot}}^{\text{UL}}(d_{\text{f},i})$ and use this point as a switching criterion on deciding whether to reuse the OB or not.

As a case study, consider a two-user scenario, where an mMS uses a subset of the frequency resources of an fMS. By equating (3.3) and (3.6) and after some manipulation, we may write

$$\left(1+\frac{P_{\text{m},i}}{I_{\text{f},j}+BN_0}\right)\left(1+\frac{P_{\text{f},j}}{I_{\text{m},i}+BN_0}\right)=\left(1+\frac{P_{\text{m},i}}{BN_0}\right)\ , \tag{3.8}$$

which, upon some further manipulation simplifies to

$$\begin{aligned}&(BN_0)^2(P_{\text{f},j}+P_{\text{m},i})+BN_0P_{\text{f},j}I_{\text{f},j}+BN_0P_{\text{m},i}I_{\text{m},i}\\&+BN_0P_{\text{m},i}P_{\text{f},j}=P_{\text{m},i}I_{\text{m},i}I_{\text{f},j}+BN_0P_{\text{m},i}I_{\text{m},i}\\&+BN_0P_{\text{m},i}I_{\text{f},j}+(BN_0)^2P_{\text{f},j}\ .\end{aligned} \tag{3.9}$$

Cancelling some common terms, we may express (3.9) as

$$\begin{aligned}&BN_0(P_{\text{f},j}I_{\text{f},j}+P_{\text{m},i}P_{\text{f},j})+(BN_0)^2P_{\text{f},j}\\&\qquad=P_{\text{m},i}I_{\text{m},i}I_{\text{f},j}+BN_0P_{\text{m},i}I_{\text{f},j}\ ,\end{aligned} \tag{3.10}$$

and dividing both sides of (3.10) by $P_{\text{m},i}$, we have

$$\frac{BN_0P_{\text{f},j}I_{\text{f},j}}{P_{\text{m},i}}+\frac{(BN_0)^2P_{\text{f},j}}{P_{\text{m},i}}+BN_0P_{\text{f},j}=I_{\text{m},i}I_{\text{f},j}+BN_0I_{\text{f},j}\ . \tag{3.11}$$

Since N_0^2 in (3.11) is typically negligible compared to other terms, it can be dropped, which yields the following interference threshold

$$I_{\mathrm{m}}^{(\mathrm{thr})} = BN_0\left(P_{\mathrm{f},j}\left(\frac{1}{P_{\mathrm{m},i}}+\frac{1}{I_{\mathrm{f},j}}\right)-1\right) . \tag{3.12}$$

Note that (3.12) gives the UL interference power threshold to be used at an fBS for achieving MSC. If the UL interference is larger than this threshold, it becomes preferable at an fBS (in the sense of maximizing the sum capacity) to avoid using the OB with the mMS. In other words, $C_{\mathrm{msc}}^{\mathrm{UL}}$ can be written as

$$C_{\mathrm{msc}}^{\mathrm{UL}} = \begin{cases} C_{\mathrm{tot}}^{\mathrm{UL}}(d_{\mathrm{f},i}) & , \text{ if } I_{\mathrm{m},i} < I_{\mathrm{m}}^{(\mathrm{thr})} \\ \tilde{C}_{\mathrm{tot}}^{\mathrm{UL}}(d_{\mathrm{f},i}) & , \text{ if } I_{\mathrm{m},i} \geq I_{\mathrm{m}}^{(\mathrm{thr})} . \end{cases} \tag{3.13}$$

Moreover, by using the related outdoor to indoor path loss models, it is also possible to explicitly obtain the corresponding threshold distance $d_{\mathrm{f},i}^{(\mathrm{thr})}$ from (3.12), by plugging the path loss equations into the power term $I_{\mathrm{m},i}$.

Since (3.12) is independent of the total bandwidth of each user, the threshold can be individually applied to each resource unit in order to decide whether to reuse that band at the femtocell or not. Therefore, (3.12) can also be applied to the case of multiple users that have scattered resource units overlapping with the resources of the femtocell spectrum. One implication of (3.12) is that if $P_{\mathrm{m},i} \to 0$, then, MSC will be achieved by using the OB.

Similar to UL scenario, DL scenario can be considered as in Fig. 3.1(b) where the spectra of mMS and fMSs are utilized as in Fig. 3.1(c). When the MSC criterion is used for DSR, the total DL capacity of all users of interest can be written as

$$C_{\mathrm{msc}}^{\mathrm{DL}} = \max\left\{C_{\mathrm{tot}}^{\mathrm{DL}}(d_{\mathrm{f},i}), \tilde{C}_{\mathrm{tot}}^{\mathrm{DL}}(d_{\mathrm{f},i})\right\} , \tag{3.14}$$

where, $C_{\mathrm{tot}}^{\mathrm{DL}}(d_{\mathrm{f},i})$ and $\tilde{C}_{\mathrm{tot}}^{\mathrm{DL}}(d_{\mathrm{f},i})$ are the total DL capacities with and without reuse of the OB at the femtocell, respectively. Dual case study of the UL scenario can also be considered for the DL scenario, where a subset of the frequency resources of an fMS is reused by an

mMS. After some similar manipulations, the DL interference threshold can be written as[3]

$$I_{\mathrm{m}}^{(\mathrm{thr})} = BN_0\left(P_{\mathrm{f},j}\left(\frac{1}{P_{\mathrm{m},i}} + \frac{1}{I_{\mathrm{f},j}}\right) - 1\right) , \tag{3.15}$$

where, $I_{\mathrm{f}}^{(\mathrm{thr})}$ expresses DL interference power threshold from fBS to mMS. If the DL interference is greater than $I_{\mathrm{m}}^{(\mathrm{thr})}$, it is worth to give up using OB in order to achieve MSC. Then, $C_{\mathrm{msc}}^{\mathrm{DL}}$ can be written as

$$C_{\mathrm{msc}}^{\mathrm{DL}} = \begin{cases} C_{\mathrm{tot}}^{\mathrm{DL}}(d_{\mathrm{f},i}) & , \text{ if } I_{\mathrm{m},i} < I_{\mathrm{m}}^{(\mathrm{thr})} \\ \tilde{C}_{\mathrm{tot}}^{\mathrm{DL}}(d_{\mathrm{f},i}) & , \text{ if } I_{\mathrm{m},i} \geq I_{\mathrm{m}}^{(\mathrm{thr})} . \end{cases} \tag{3.16}$$

Similar to the UL scenario, corresponding threshold distance $d_{\mathrm{m},i}^{(\mathrm{thr})}$ can also be obtained explicitly through the related path loss formula by plugging the power term $I_{\mathrm{m},i}$ into (3.15).

In order to better understand how the threshold may be used for MSC, consider a case study as illustrated in Fig. 3.1 with two users, where the fBS is located at the center of a 15 m $\times$15 m apartment that has 10 dB wall penetration loss, mBS is located at $d_{\mathrm{mBS}} = 500$ m or $d_{\mathrm{mBS}} = 1000$ m away from the fBS, fMS is located 7 m away from the fBS, and the mMS is located on a line between the fBS and the mBS. Let $N_{\mathrm{m}} = 2$ and $N_{\mathrm{f}} = 10$ resource units be utilized at the macrocell and the femtocell, respectively, where the femtocell fully occupies a 5 MHz spectrum. For the UL scenario, the mMS causes significant interference to (and receives significant interference from) the fMS while it is closer to the fBS. For the DL scenario, power level of the received interference signal at the mMS decreases while the mMS moves away from the fBS to mBS. On the other hand, the interference signal power at the fMS from the mBS is assumed constant.

Fig. 3.3 and Fig. 3.4 illustrate the UL sum-capacity and the UL femtocell capacity for $d_{\mathrm{mBS}} = 500$ m and $d_{\mathrm{mBS}} = 1000$ m, respectively, for fBS-mMS distances from 0 m up to 60 m in a closed access implementation. With DSR, when the mMS is relatively closer to the fBS, it is assumed that the interference can be detected through perfect spectrum

[3]Note that compared to (3.12), the received power and interference values in (3.15) correspond to the reverse link, as illustrated in Fig. 3.1.

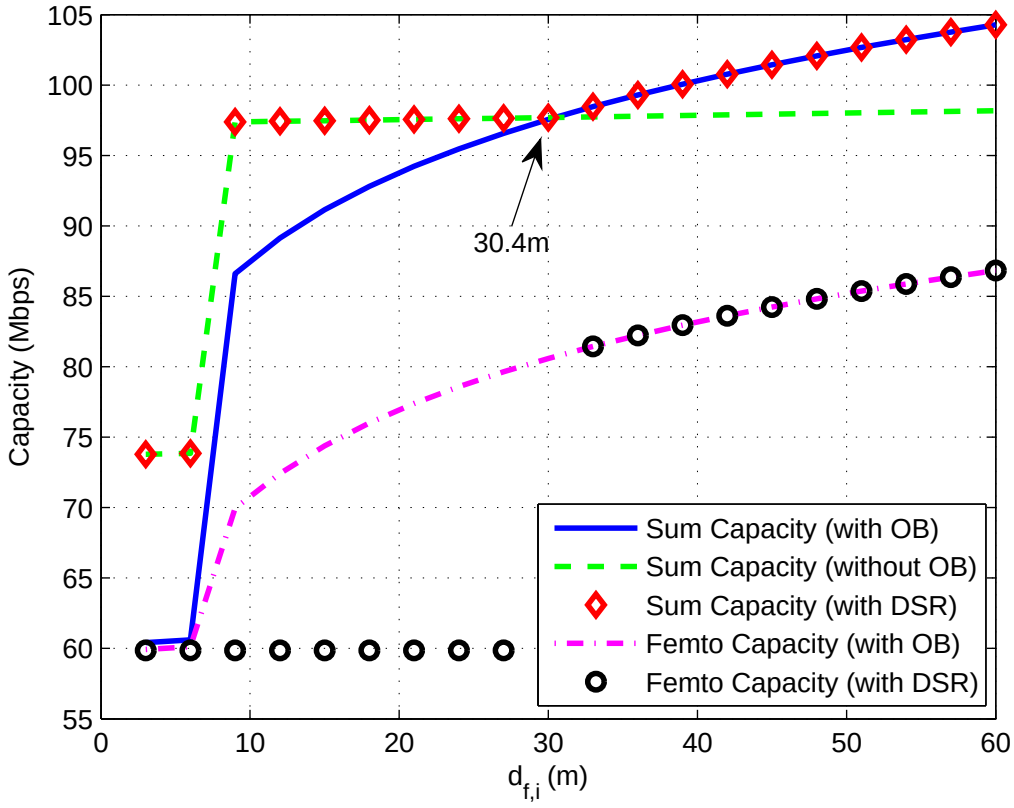

Figure 3.3 UL sum-capacity and femtocell capacity with DSR ($P_{\mathrm{f,j}} = 10$ dBm, $P_{\mathrm{m,i}} = 20$ dBm, $d_{\mathrm{mBS}} = 500$ m).

sensing, and the femtocell abstains from reusing the OB. In this case, even though the fMS capacity degrades due to the use of a smaller bandwidth, the total UL capacity improves due to reduced interference. In other words, rather than wasting the OB for both users, it is utilized interference-free by the mMS. The improvement in the sum-capacity with DSR is more obvious for smaller d_{mBS}. Both sum-capacity and femtocell capacity have a sharp increase at around $d_{\mathrm{mBS}} = 7.5$ m, which is due to the existence of the building wall. The $d_{\mathrm{f},i}$ analytically computed using the threshold value in (3.13) is also indicated in Fig. 3.3 and Fig. 3.4, and match well with the crossing point of the closed access sum-capacity with and without reuse of the OB at the femtocell.

The DL results in Fig. 3.5 and Fig. 3.6 show that similar to the UL, there is a cross-over distance $d_{\mathrm{f},i}$ where reuse of the OB no longer becomes preferable for maximizing the

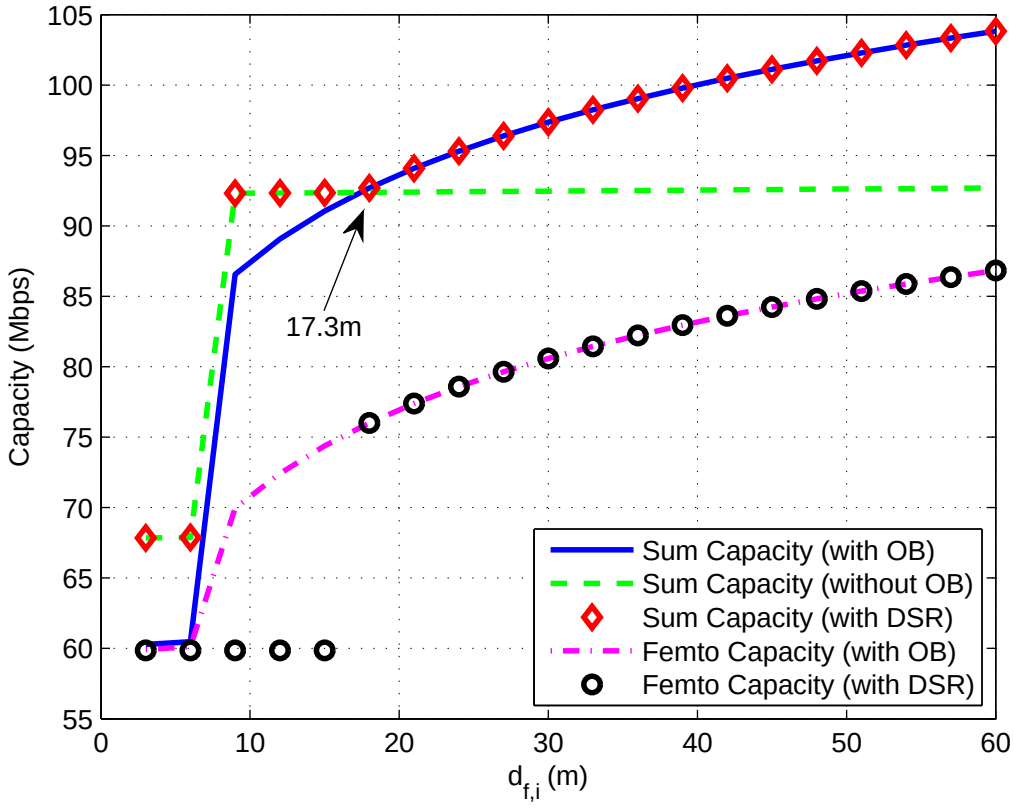

Figure 3.4 UL sum-capacity and femtocell capacity with DSR ($P_{\mathrm{f,j}} = 10$ dBm, $P_{\mathrm{m,i}} = 20$ dBm, $d_{\mathrm{mBS}} = 1000$ m).

sum-capacity. Again, the $d_{\mathrm{f},i}$ obtained from (3.16) matches well with the crossing point of CSG sum capacity with and without reuse of the OB at the femtocell. The sum-capacity improvement due to using DSR is also larger when the mBS is closer to the femtocell.

3.2.2 Minimum Macrocell Loss

One of the primary goals of femtocell deployments is to cause minimal capacity degradation to the existing macrocell network while enhancing the capacity of users that are connected to the femtocells. Interference impact from the femtocell to the mMSs is typically given higher priority compared to the interference from the mMSs to the femtocell [17]. Therefore, maximizing the sum capacity may not always be acceptable if the femtocell interference on the mMSs is intolerable. In particular, for the scenarios where the fMSs already

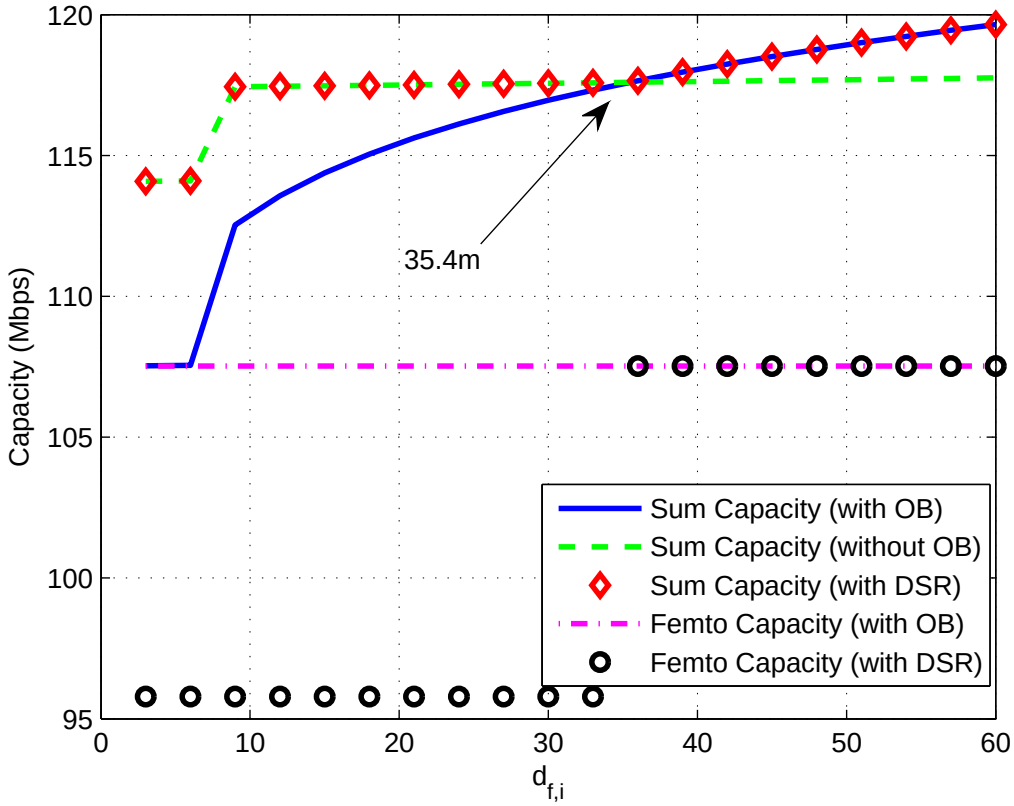

Figure 3.5 DL sum-capacity and femtocell capacity with DSR ($P_{\mathrm{f,j}} = 10$ dBm, $P_{\mathrm{m,i}} = 40$ dBm, $d_{\mathrm{mBS}} = 500$ m).

have the spectrum resources that are not interfered, releasing the OB at the femtocell may significantly improve the capacity of the mMSs with limited relative impact on the capacity of the fMSs.

On the other hand, there may also be scenarios where capacity augmentation at the mMS causes a considerable capacity loss at the femtocell. This loss can be expressed as

$$L_{\mathrm{f}}^{\mathrm{UL}}(d_{\mathrm{f},i}) = \sum_{j \in \mathcal{S}_{\mathrm{f}}} \left(C_{\mathrm{f},j}^{\mathrm{UL}}(d_{\mathrm{f},i}) - \tilde{C}_{\mathrm{f},j}^{\mathrm{UL}}(d_{\mathrm{f},i}) \right) , \tag{3.17}$$

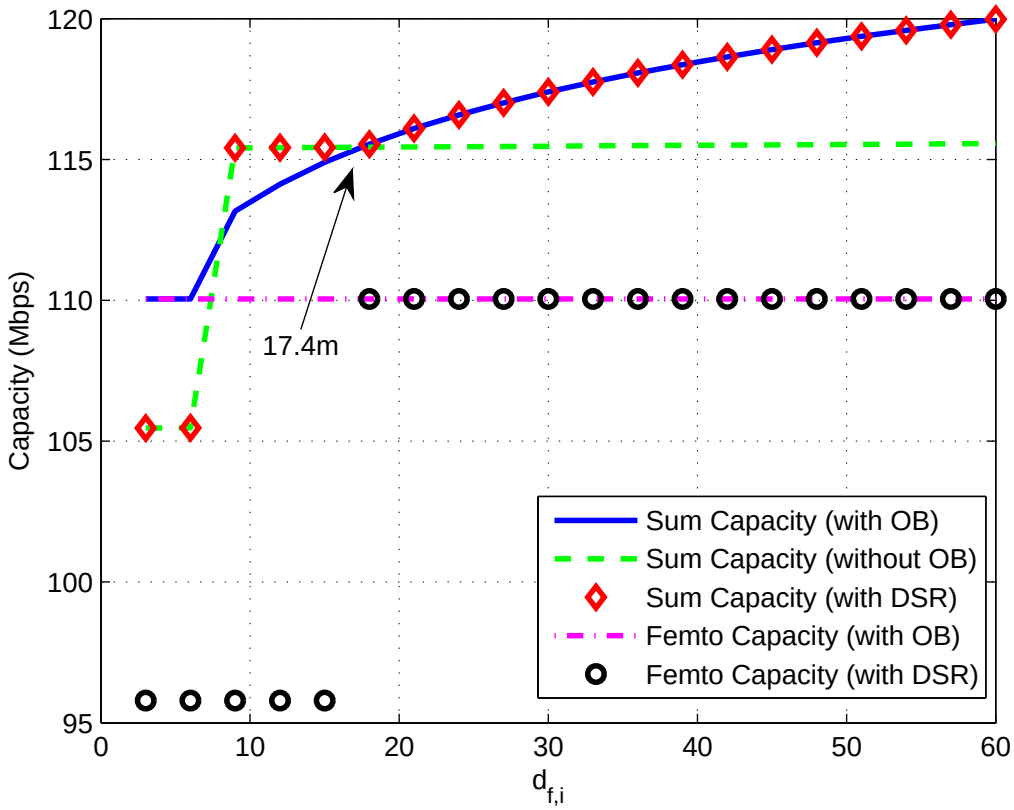

Figure 3.6 DL sum-capacity and femtocell capacity with DSR ($P_{\mathrm{f,j}} = 10$ dBm, $P_{\mathrm{m,i}} = 40$ dBm, $d_{\mathrm{mBS}} = 1000$ m).

where the ratio of the capacity loss that a femtocell observes is[4]

$$\zeta_{\mathrm{f}} = \frac{L_{\mathrm{f}}^{\mathrm{UL}}(d_{\mathrm{f},i})}{\sum_{j\in\mathcal{S}_{\mathrm{f}}} C_{\mathrm{f}}^{\mathrm{UL}}(d_{\mathrm{f},i})} \ . \tag{3.18}$$

Note that $L_{\mathrm{f}}^{\mathrm{UL}}(d_{\mathrm{f},i})$ depends on the femtocell power over an OB, especially the mMSs who are victim of closed access policy with a severe interference ($P_{\mathrm{m},i} \leqslant I_{\mathrm{f},j}$). However, it is mostly driven by the ratio of OB which is defined as OB over the total femtocell bandwidth.

In this section, a second metric that considers a minimum macrocell loss (MML) is evaluated. Proposed metric takes into account the capacity loss of an mMS who is victim

[4]Since there may typically be single fMS user per femtocell, it may be assumed that (3.18) is also the ratio of the capacity loss per fMS ($\zeta_{\mathrm{f},j}$).

of closed access policy. The loss can be written as

$$L_{\mathrm{m},i}^{\mathrm{UL}}(d_{\mathrm{f},i}) = \tilde{C}_{\mathrm{m},i}^{\mathrm{UL}}(d_{\mathrm{f},i}) - C_{\mathrm{m},i}^{\mathrm{UL}}(d_{\mathrm{f},i}) \ , \tag{3.19}$$

where the ratio of the capacity loss that an mMS observes is

$$\eta = \frac{L_{\mathrm{m},i}^{\mathrm{UL}}(d_{\mathrm{f},i})}{\tilde{C}_{\mathrm{m},i}^{\mathrm{UL}}(d_{\mathrm{f},i})} \ . \tag{3.20}$$

Then the decision metric based on the MML criterion can be written as

$$C_{\mathrm{mml}}^{\mathrm{UL}}(d_{\mathrm{f},i}) = \begin{cases} C_{\mathrm{m},i}^{\mathrm{UL}}(d_{\mathrm{f},i}) & , \text{ if } \eta \ < \ \eta^{\mathrm{thr}} \\ \\ \tilde{C}_{\mathrm{m},i}^{\mathrm{UL}}(d_{\mathrm{f},i}) & , \text{ if } \eta \ \geq \ \eta^{\mathrm{thr}} \ , \end{cases} \tag{3.21}$$

where η^{thr} $(0 \leqslant \eta^{\mathrm{thr}} \leqslant 1)$ indicates tolerance level of an mMS to capacity loss. For mMSs that are vulnerable to capacity loss, η^{thr} is close to 0. When η^{thr} is closer to 1, the mMS is more tolerant to capacity loss. In other words, $\eta^{\mathrm{thr}} = 1$ shows that the mMS has full tolerance and OB will be employed for any case, whereas $\eta^{\mathrm{thr}} = 0$ indicates that the mMS has no tolerance to capacity loss and OB reuse cannot be employed. Note that η is independent from OB meaning that the loss observed at mMS is only due to degradation of its SINR value. Fig. 3.7 depicts the ζ_{f} values according to different OB ratios for various fMS powers. It also shows that effect of OB ratio has more influence on ζ_{f} after the $I_{\mathrm{f},j}$ dominates the $P_{\mathrm{m},i}$. Fig. 3.7 also shows corresponding η values for each fMS power. An illustrative example is shown in Fig. 3.7 whether the OB will be used or not with respect to $\eta^{\mathrm{thr}} = 0.5$.

3.2.3 Minimum Effective Interference

The guideline document prepared by ITU specifies an interference over thermal noise (IoT) parameter which indicates effective interference level received at the base station [18].

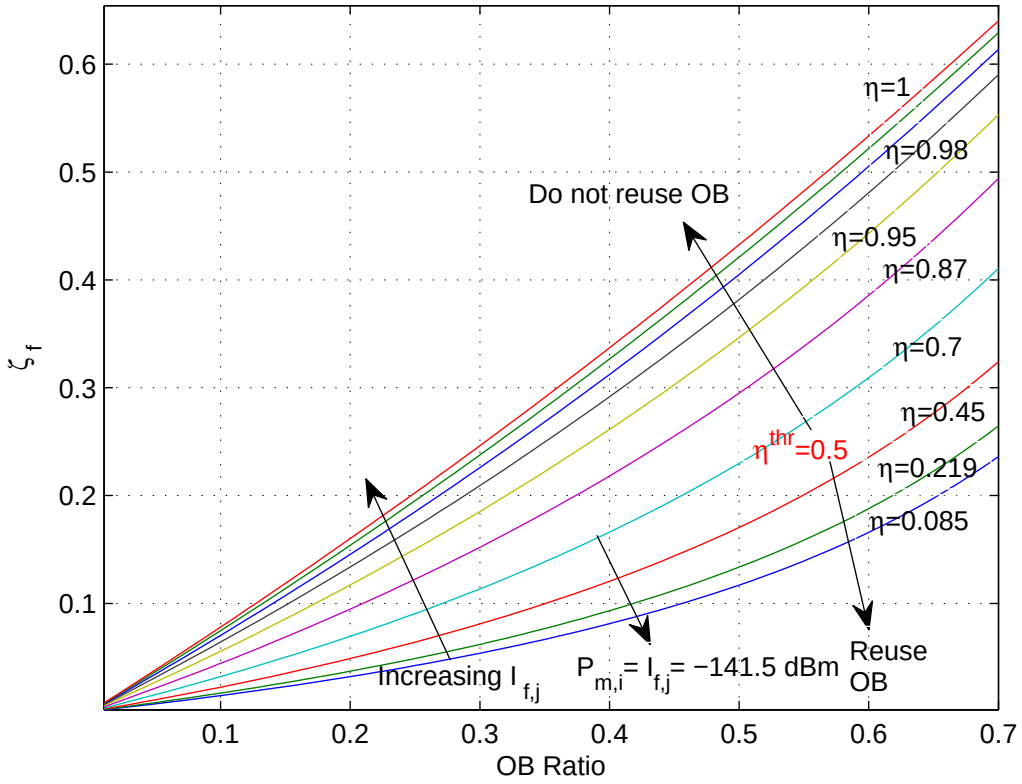

Figure 3.7 Femtocell capacity loss ratio (ζ_{f}) vs. overlapped band (OB) ratio ($P_{\mathrm{m},i} = -141.5$ dBm and $I_{\mathrm{f},j} = \{-111.5, -116.5, ..., -156.5\}$ dBm).

An easy method to calculate IoT is provided in [19] and it can be written as

$$IoT_{\mathrm{m}} = \frac{\sum_{j \in \mathcal{S}_{\mathrm{f}}} I_{\mathrm{f},j} + BN_0}{BN_0}, \tag{3.22}$$

where IoT_{m} represents the total fMS interference over thermal noise level at the mBS over the transmission bandwidth B.

The IoT parameter may be used to detect the femtocell interference at the mMSs. If the interference level is large, the mMSs may signal this information to the relevant femtocell[5], which may re-schedule its fMSs to different bands to prevent interference. The IoT value

[5]This may be achieved using the X2 interface in LTE, or, the mMS may directly relay the interference coordination information between mBS and fBS over the air [20], [21].

for an mMs can be calculated as

$$IoT_{\mathrm{m},i} = \frac{I_{\mathrm{m},i} + BN_0}{BN_0}, \tag{3.23}$$

where $IoT_{\mathrm{m},i}$ represents the all fBS interferences over thermal noise level at the i^{th} mMS over the transmission bandwidth B. Then, minimum effective interference (MEI) decision metric based upon IoT can be written as

$$C_{\mathrm{mei}}^{\mathrm{DL}} = \begin{cases} C_{\mathrm{m},i}^{\mathrm{DL}} & , \text{ if } IoT_{\mathrm{m},i} < I_{\mathrm{thr}} \\ \tilde{C}_{\mathrm{m},i}^{\mathrm{DL}} & , \text{ if } IoT_{\mathrm{m},i} \geq I_{\mathrm{thr}} \ , \end{cases} \tag{3.24}$$

where I_{thr} shows tolerable total femtocell interference level over noise for i^{th} mMS. An exemplary value for I_{thr} to be employed in IMT-Advanced standards is specified as equal to or less than 10 dB by ITU [18]. The mMS can conclude to avoid reusing the OB by measuring its IoT level without needing any other network parameter.

3.3 Simulation Results

Simulations are performed to evaluate the potential gains of the proposed techniques in MATLAB and most of the key simulation parameters are selected based on [8] and are summarized in Table 2.3. The indoor/outdoor path loss models as specified in ITU P.1238 and ITU P.1411 are utilized. A macrocell/femtocell scenario as in Fig. 2.3 and Fig. 2.4 are considered where an mBS is located at the center of the cell (shown with triangle). Buildings (squares) are uniformly scattered whereas 150 mobile users are distributed such a way that at least 82% of the users are indoor and 18% of the users are outdoor [6]. SINR value based cell selection is employed unless the users do not violate closed access policy. Idle femtocells (with no users) are detected and disabled by setting their transmitting power to zero in order to minimize interference. Results are averaged over 200 different realization.

In order to simulate the closed access scheme, at least 30% of indoor users are forced to register to macrocell although their signal strengths are good enough to register to the

femtocells in their vicinity. Presented techniques are simulated in order to overcome capacity reduction due to reuse of highly interfered OBs. Proposed metrics MSC, MML and MEI are simulated along with OA and closed access for the purpose of comparison.

Median capacity comparison between OA and closed access deployment schemes is provided in Table 3.1. Note that macrocell capacity reduction between OA and closed access is not only due to the increase in interference observed by mMSs but also because of the increase in number of mMSs over the same spectrum resource. Table 3.1 also shows that median capacity is maximized by employing sum capacity maximization metric (MSC).

The capacity CDFs of mMSs and fMSs with and without the proposed DSR techniques are depicted in Fig. 3.8 and Fig. 3.9. Only the mMSs that are within the vicinity of femtocells are considered in the capacity CDFs. To this end, the victim mMSs are detected using one of the three metrics discussed in the previous section. Therefore, no DSR with MSC-detected, MML-detected, and MEI-detected refer to the schemes without DSR and where the mMS users are detected based on one of the three different criteria[6]. The superior mMS CDF curve seems to belong to MEI where I_{thr} is equal to 5 dB, however approximately 30% of detected mMSs are found to suffer from low capacity although their capacity is good. On the other hand, all mMSs detected by MML criteria, where $\eta^{\text{thr}} = 0.5$, suffer from low capacity. The enhancement in mMS capacity comes at the expense of femtocell user capacity loss. Fig. 3.9 shows the corresponding capacity loss in fMSs for each metric. The difference between the CDF values for a given capacity may vary between 2.5%-3.5% for proposed metrics.

The capacity loss that fMS observes is heavily dependent on the OB that fMS does not reuse. Therefore, for the scenario where the number of mMSs in the macrocell is much more than the number of fMSs in a femtocell, the effect of releasing the OB is bearable to the fMSs. On the other hand, for a scenario where the number of mMS in a macrocell is comparable to the number of fMSs in a femtocell, releasing the OB affects the fMSs more severely. Fig. 3.10 and Fig. 3.11 show mMS capacity improvement and corresponding fMS

[6]Note that the threshold metrics used in the simulations are representative values based on educated guess and further optimizations of these values are possible.

Table 3.1 Comparison of median capacities (in mbps) w.r.t. different metrics.

Users (%)	Closed Access	DSR (MSC)	DSR (MML, η^{thr}=0.5)	DSR (MEI, I_{thr}=**5 dB**)	Open (%) Access
All	25.09	25.84	25.48	25.68	31.00
Indoor (78)	31.81	32.76	32.34	32.47	38.85
Outdoor (22)	1.91	2.00	1.91	2.12	3.86
Femto (52)	46.67	47.74	46.80	47.40	39.8 (76)
Macro (48)	1.03	1.87	1.82	1.92	3.79 (24)

capacity loss where macrocell has 4 users and each femtocell has up to 4 users. In Fig. 3.10 all detected mMSs, according to MML method, suffer from low capacity whereas only 85% of the detected users have desperate capacity in MSC method. Thus, the favorable mMS CDF curve can be decided by the metric which favors only the mMSs who deeply suffer (e.g. MML (η^{thr}=0.5)) . The fMS capacity loss that corresponds to Fig. 3.10 is illustrated in Fig. 3.11 where the loss due to the releasing OB is quite considerable. Various $\zeta_{\text{f},j}$ values are also marked for three methods in Fig. 3.11 where OB ratio is around 25%. It can be seen that marked $\zeta_{\text{f},j}$ in Fig. 3.11 are not exceeding the ζ_{f} values in Fig. 3.7 for the OB ratio is 25%.

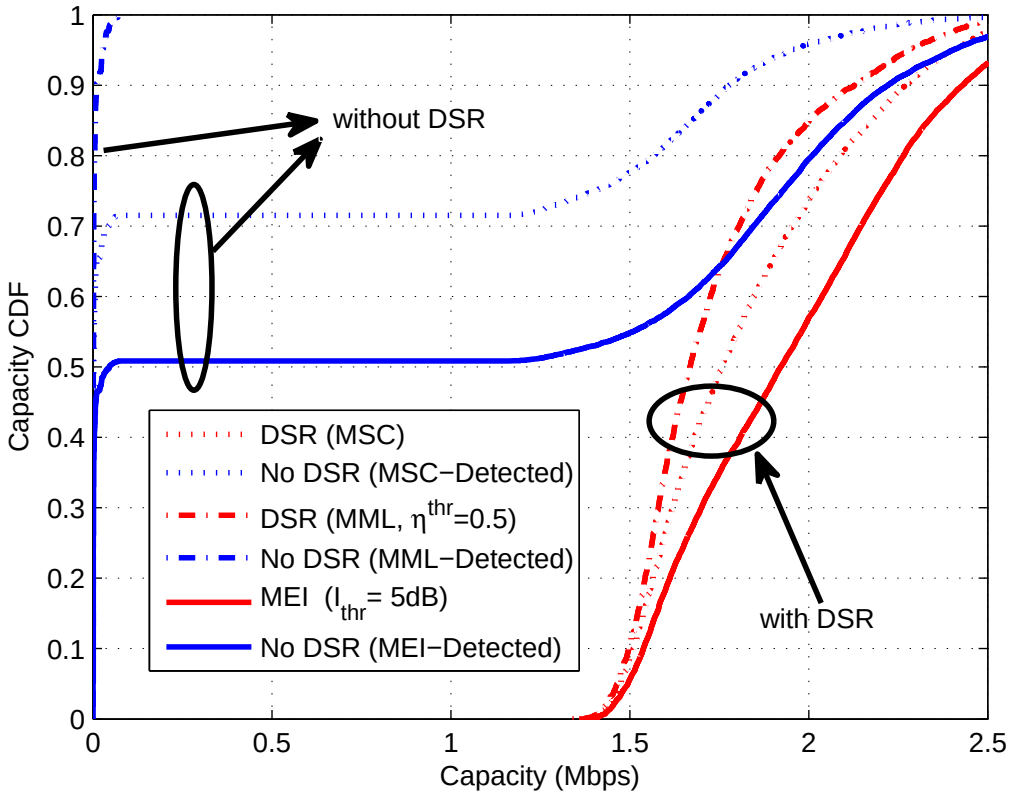

Figure 3.8 Comparison of macrocell user capacity CDFs (in dense mMS environment).

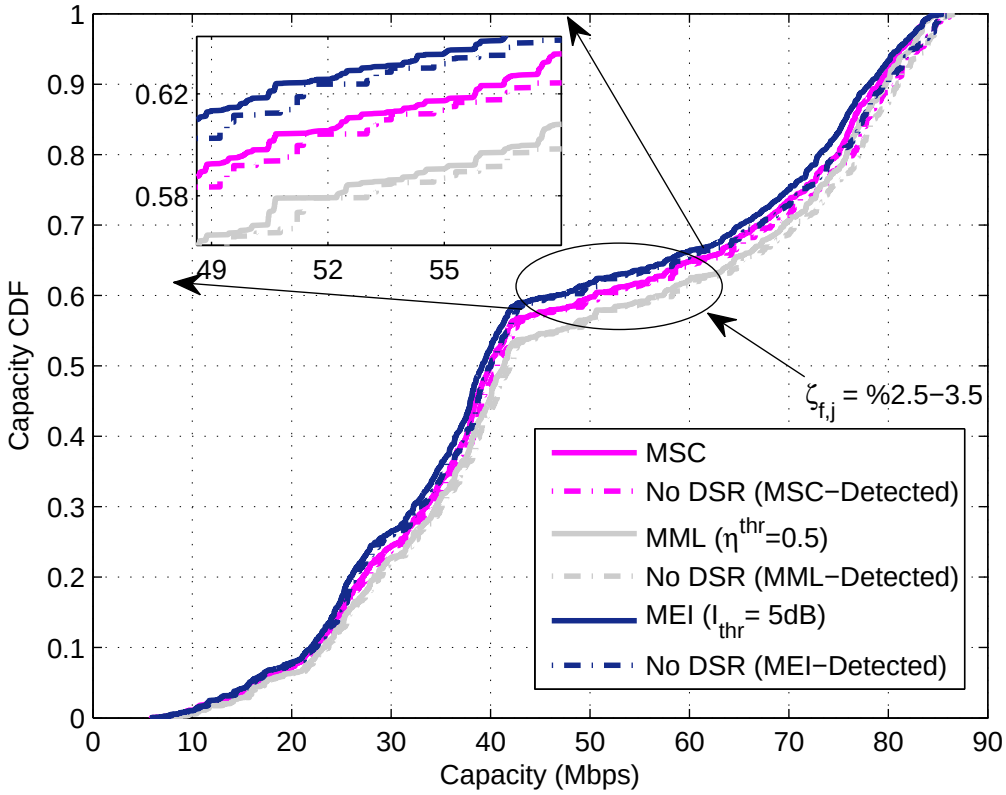

Figure 3.9 Comparison of femtocell user capacity CDFs with $\zeta_{f,j}$ value (in dense mMS environment).

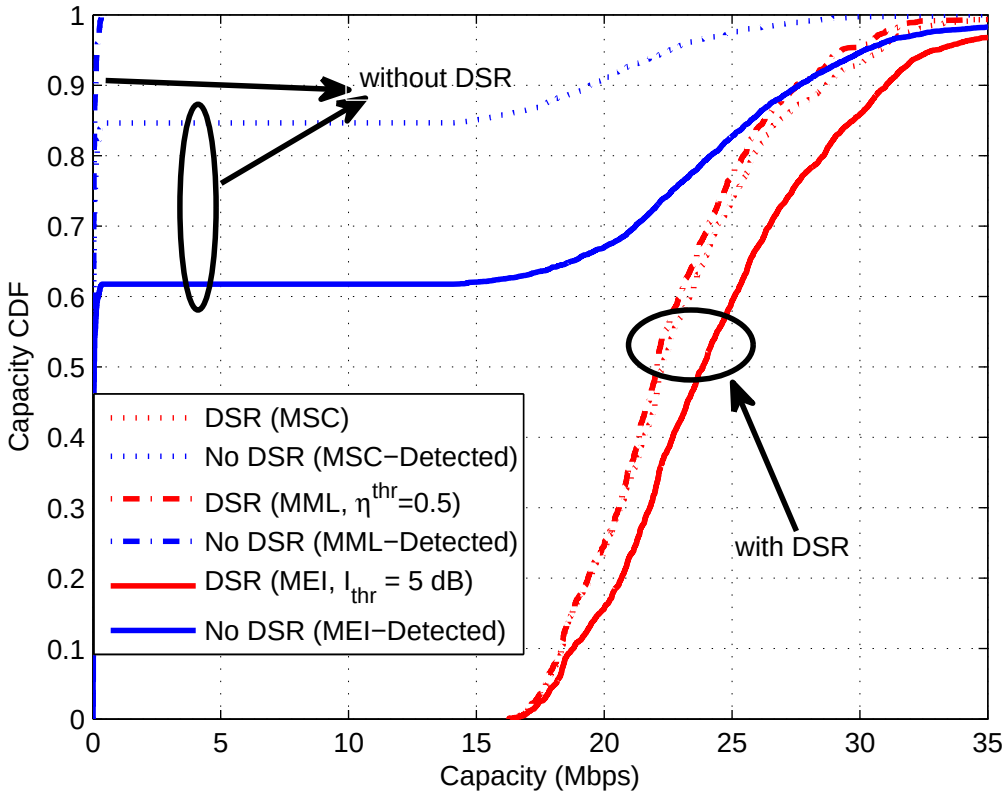

Figure 3.10 Comparison of macrocell user capacity CDFs (in sparse mMS environment).

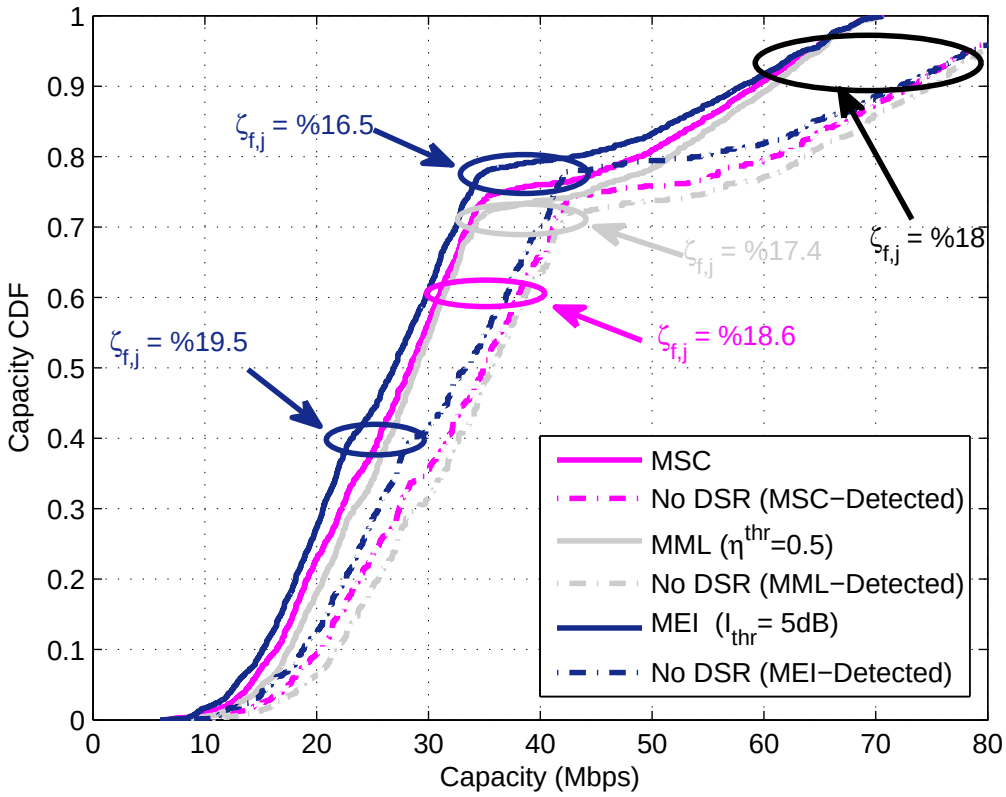

Figure 3.11 Comparison of femtocell user capacity CDFs with various $\zeta_{f,j}$ values (in sparse mMS environment).

CHAPTER 4

OPEN ACCESS FEMTOCELLS

One of the major concerns in femtocell network deployment is interference mitigation. Due to the use of same spectrum resource over two tiered networks at the same time, significant interference is introduced to the networks. In order to combat the interference or at least reduce the interference to an acceptable level, several methods can be employed such as transmission power control, spectrum resource partitioning, and application of different accessing schemes.

First, power control has already been employed to macrocell network in order to mitigate so-called near-far effect for cell-edge users [22]. In femtocell networks, depending on the fMS location, fMS adapts its transmission power in such a way that it causes minimal interference to the network while communicating with the fBS. This adaptation allows fMS to reduce inter cellular interference (among the femtocells) and intra cellular interference (between femtocell to macrocell).

Second, spectrum resource portioning is also used for interference mitigation in two tired networks. It can be done in three ways:

- Co-channel spectrum allocation : It is a spectrum allocation method where the spectrum resource is used universally in entire networks by allowing the interference among those networks (both femtocell to femtocell and femtocell to macrocell).

- Dedicated spectrum allocation : Dedicated spectrum allocation prevents the interference from femtocell to macrocell and vice versa by assigning a certain portion of spectrum resource to the femtocell networks; however, femtocell to femtocell interference still remains. In order to achieve further reduction in femtocell to femtocell

interference, femtocells' spectrum resources are subdivided into several more pieces so that certain femtocell groups are not interfering with each other [23].

- Hybrid spectrum allocation : Another way to utilize the spectrum resource is hybrid spectrum allocation where the resource is organized in such a way that one part of the spectrum only belongs to macrocell usage, another part only belongs to femtocells usage. There is also third part belonging to the users who are allowed to switch among the networks [24].

Third, accessing scheme used in femtocell network deployment directly affects the interference level in the environment. In closed access (closed subscriber group (CSG)) femtocell, the number of mMSs can join a particular femtocell network is limited. So, any user that is not listed as permitted user causes and receives high interference femtocell. On the other hand, for open access (OA) femtocell networks, any user equipment (UE) receiving better link quality from femtocell is granted as femtocell user so that interference between femtocell to macrocell is reduced. However, there are some drawbacks related to OA that should be mentioned [2, 3, 23]

- OA introduces to the network more signaling due to hand off negotiation process
- Security issues
- Augmentation in the femtocell backhaul burden
- Pre-paid femtocell owners are not willing to receive non-subscriber user unless they are given earnings

In this section OA network is analyzed. For OA femtocell network, any UE above the cell selection criterion threshold will be granted as subscriber to the base station of interest. Cell selection can be done based on received signal strength (RSS), capacity, and interference level of the users.

In OA femtocell deployment scheme, compared to CSG mode, the femtocell has more subscribers since some of the mMSs hand-off to the femtocell. Although available bandwidth

per user decreases, the interference level that the femtocell observes decreases as well because the mMSs who register to the femtocell cause the strongest interference to the femtocell. Reduction on the interference can cover the bandwidth reduction per fMS and increase femtocell throughput. Moreover, macrocell serves less number of mMS which results in mMSs to have much wider bandwidth (so called off-loading effect) and it observes less interference. Regarding the overall system throughput, it has been showed via example simulations in [11–13] that OA provides better results.

4.1 Capacity Analysis of Open Access Scheme in Two Tiered Networks

The role that femtocell plays is to improve cellular networks capacity according to dedicated and co-channel resource portioning methods is presented. Macrocell capacity without femtocells is also given for the purpose of comparison.

4.1.1 Macrocell Capacity without Femtocell Deployment

Assuming that M mMSs are randomly distributed to the macrocell illustrated in Fig. 2.3 and they are communicating with the mBS. Also, assuming total available spectrum for the macrocell B_{tot} is equally scheduled to its users. Then the capacity equation where femtocell is not employed can be expressed as

$$C_{\text{m,i}} = \frac{B_{\text{tot}}}{M} log\left(1 + \frac{P_{\text{m,i}}}{N_0(B_{\text{tot}}/M)}\right), \tag{4.1}$$

where $P_{\text{m,i}}$ is the received power over transmission bandwidth ($B_{\text{m,i}} = B_{\text{tot}}/M$) of i^{th} mMS and N_0 represents the noise power per hertz.

It can be concluded from (4.1) that capacity improvement can be achieved by increasing the transmission bandwidth of mMS ($B_{\text{m,i}}$) via either having smaller M or larger B_{tot} or increasing the received power ($P_{\text{m,i}}$). However, RSS of the mBS observed by indoor users is significantly lower than the RSS experienced by outdoor users due to the wall penetration loss as in depicted in Fig. 2.3 where indoor coverage is poor. Femtocells can be remedy to indoor users' RSS problem by deploying them within the houses/offices so that RSS as well

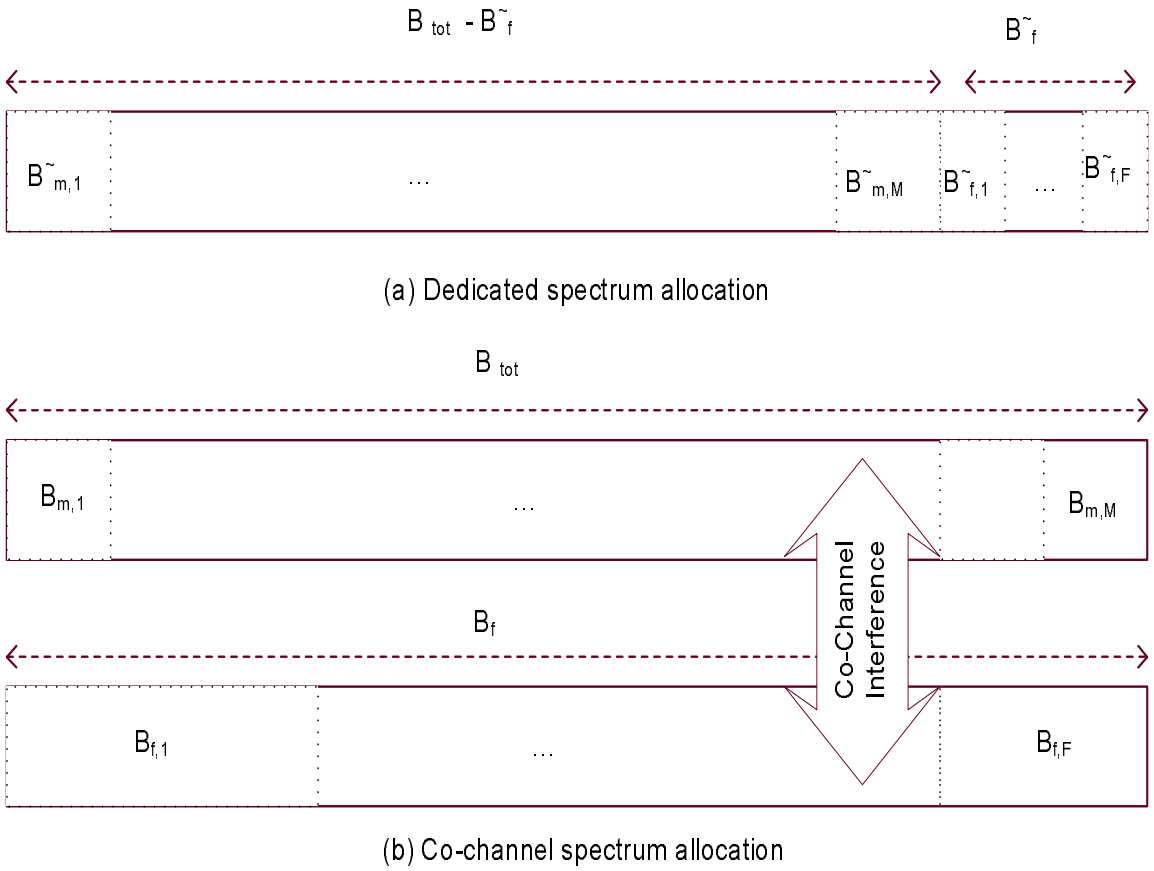

Figure 4.1 (a) Dedicated spectrum allocation vs. (b) Co-channel spectrum allocation of femtocell and macrocell networks.

as capacity of indoor users can be increased as in depicted in Fig. 2.4 where indoor coverage is increased.

4.1.2 Capacity Improvement with Femtocell Deployment

Dedicated and co-channel spectrum resource usage are presented.

4.1.2.1 Dedicated Spectrum Resource Allocation

The spectrum resources of femtocell and macrocell are isolated by assigning each of them a split spectrum as illustrated in Fig. 4.1(a). Interference between femtocell and macrocell is substantially eliminated however the interference among femtocells still remains. Also, spectrum utilization is not efficiently employed by dividing the available spectrum resource.

The capacity of an mMS with dedicated channel assignment can be written as

$$\tilde{C}_{\mathrm{m},i} = \frac{B_{\mathrm{tot}} - \tilde{B}_{\mathrm{f}}}{\tilde{M}} \log\left(1 + \frac{P_{\mathrm{m},i}}{N_0(B_{\mathrm{tot}} - \tilde{B}_{\mathrm{f}})/\tilde{M}}\right), \tag{4.2}$$

where $\tilde{B}_{\mathrm{f}}$ is the bandwidth assigned to femtocell networks and $\tilde{M}(\tilde{M} < M)$ is the number of mMS registered to mBS. It can be deducted from (4.1) and (4.2) that with the deployment of femtocells there is a reduced amount of available spectrum for the macrocell network. However, also, some of the users $(M - \tilde{M})$ are relieved of to the femtocell networks, and they no longer connect to the macrocell to use its frequency resources. Thus, macrocell capacity can be improved by deploying the femtocells with smaller $\tilde{B}_{\mathrm{f}}$ and $\tilde{M}$.

On the femtocell side, remaining of the spectrum resource (B_{f}) is used by femtocell. The capacity of an fMS where equal bandwidth scheduler is employed can be expressed as

$$\tilde{C}_{\mathrm{f},i} = \frac{\tilde{B}_{\mathrm{f}}}{F} \log\left(1 + \frac{P_{\mathrm{f},i}}{N_0(\tilde{B}_{\mathrm{f}}/F)}\right), \tag{4.3}$$

where F is the number of the users per femtocell and the fMS receives the signal at a power of $P_{\mathrm{f},i}$ from fBS. Comparing (4.3) with (4.1), although the bandwidth per user $\left(\tilde{B}_{\mathrm{f},i} = \tilde{B}_{\mathrm{f}}/F\right)$ may be similar to the bandwidth of indoor macrocell users without any femtocell deployment, the received powers $P_{\mathrm{f},i}$ would typically expand considerably with femtocell deployments, thus improving the capacity of indoor users.

4.1.2.2 Co-channel Spectrum Resource Allocation

Femtocell are given to use entire available spectrum resource which results in the utilization of the spectrum more efficient manner. Co-channel spectrum resource allocation enables both femtocell and macrocell users to have a larger bandwidth ($B_{\mathrm{m},i} > \tilde{B}_{\mathrm{m},i}$ and $B_{\mathrm{f},i} > \tilde{B}_{\mathrm{f},i}$, respectively) as depicted in Fig. 4.1(b). Furthermore, for the handover purposes it becomes easier for an mMS to search for cells in same frequency bands. On the other hand, it introduces to the network co-channel interference so both femtocells and macrocell observe interference from each other.

When the spectrum resource is universally used by both femtocells and macrocell, the channel capacity of an mMS can be written as

$$\widehat{C}_{\mathrm{m},i} = \frac{B_{\mathrm{tot}}}{\tilde{M}} \log\left(1 + \frac{P_{\mathrm{m},i}}{I_{\mathrm{f}} + (B_{\mathrm{tot}}/\tilde{M})N_0}\right), \tag{4.4}$$

where I_{f} is the total interference observed from all close by femtocell networks. Comparing (4.4) with (4.2), it is observed that the bandwidth available per user improves with co-channel deployment (i.e., $B_{\mathrm{m},i} > \tilde{B}_{\mathrm{m},i}$). However, the mMSs also observe interference I_{f} from nearby femtocell networks, which may degrade the capacity if it is significant. Therefore, whether the capacity improves or not with respect to a dedicated channel scenario depends jointly on $\tilde{B}_{\mathrm{f}}$ and I_{f}. On the other hand, typically there is only little improvement in average macrocell user bandwidth when co-channel deployments is considered instead of dedicated channel deployment. Hence, it is typically the case that the capacity of macrocell users would be larger with dedicated channel deployments due to interference problems.

Similarly, comparing (4.4) with (4.1), whether the capacity improves or not for co-channel deployment with respect to a no-femtocell scenario depends jointly on M and I_{fem}. If more users can be off-loaded to femtocells, we have smaller M, which may overweigh the impact of interference and improve the capacity of remaining macrocell users.

On the other hand, the capacity of an fMS user with co-channel deployment can be written as

$$\widehat{C}_{\mathrm{f},i} = \frac{B_{\mathrm{f}}}{F} \log\left(1 + \frac{P_{\mathrm{f},i}}{I_{\mathrm{m}} + N_0(B_{\mathrm{f}}/F)}\right), \tag{4.5}$$

where $B_{\mathrm{f}} = B_{\mathrm{tot}} \gg \tilde{B}_{\mathrm{fem}}$, which implies significant increase in available bandwidth per femtocell user. This comes at the expense of interference I_{m} observed from macrocell users and the mBS. Since bandwidth affects the channel capacity linearly, and interference affects the channel capacity through the logarithm function, as also discussed by several other work in the literature ([2, 12, 13, 25]) co-channel deployments of femtocells typically result in

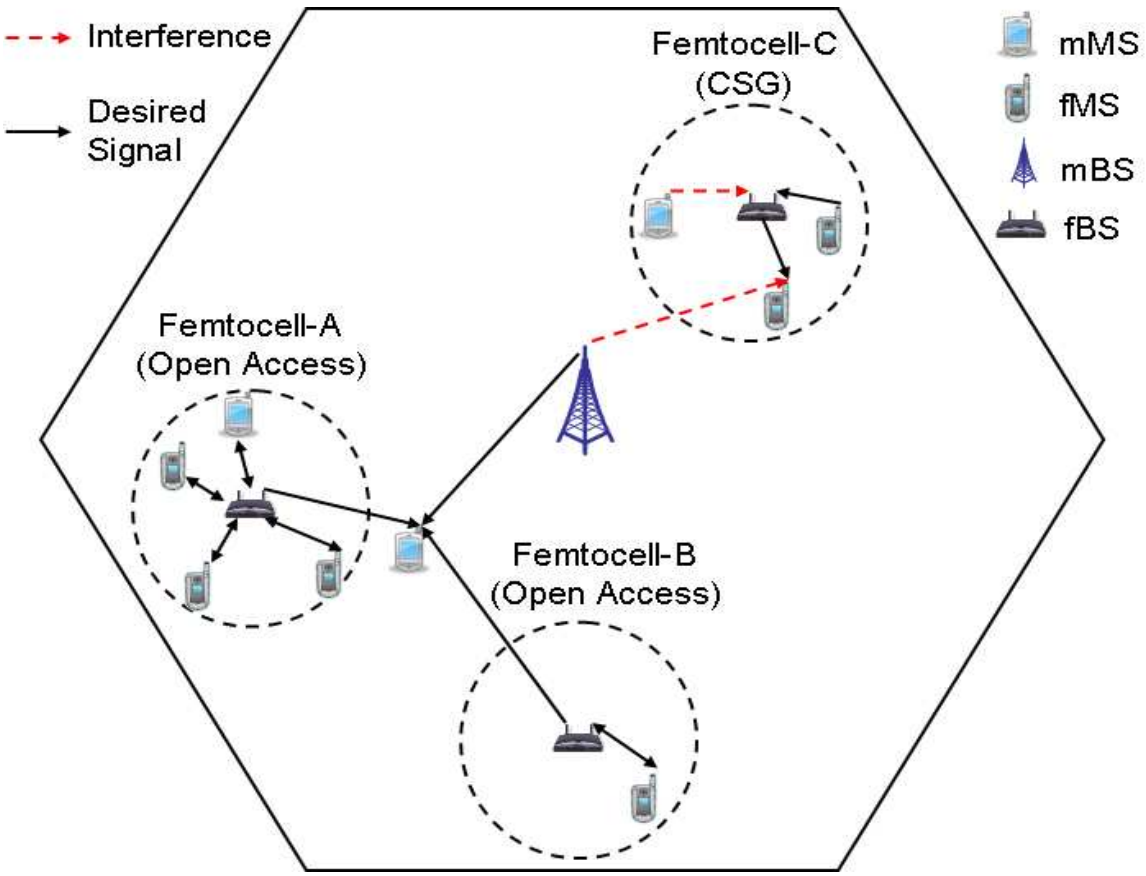

Figure 4.2 Open access and closed access modes of femtocell networks.

better overall capacities compared to dedicated channel deployments. These observations will also be verified through computer simulations in Section 4.3.

4.2 Open Access with Load Balancing (OA-LB)

For the open access mode, the mMS is allowed to make a hand-off to the femtocell. How the hand-off is triggered is a critical optimization problem for the throughput of the femtocell and macrocell users. Typically, the cell with the RSS is selected for hand-off (see e.g., [26]) in the prior-art, where, the cell with the best signal quality can be written as

$$\hat{i} = \arg\max_{i} \left\{ P_{\mathrm{m},i} \right\} , \tag{4.6}$$

where i denotes the candidate cell index, $P_{\mathrm{m},i}$ is the received DL signal power from cell-i, and the mMS eventually makes a hand-off to the cell with the best signal quality.

However, interference and bandwidth are two other critical parameters affecting the capacity of MSs, and should be also taken into account [27]. For example, for the mMS in Fig. 4.2, the link quality from Femtocell-A and the mBS may be better than the link quality from Femtocell-B; however, Femtocell-A is overloaded with several users, and there is only a single user in Femtocell-B. Therefore, due to the availability of larger spectrum resources, Femtocell-B may provide better capacity to the mMS compared to Femtocell-A or the macrocell. The capacity-maximizing cell selection for the mMS may simply be formulated as[1]

$$\hat{i} = \arg\max_{i} \left\{ C_{\mathrm{m},i} \right\} , \tag{4.7}$$

where $C_{\mathrm{m},i}$ denotes the resulting capacity of the mMS if it makes a hand-off to cell-i. Note that (4.7) does not only take the link quality into account, but also the available bandwidth and the interference. The advantages of (4.7) include 1) The spectrum is more fairly distributed among macrocell and femtocell users, 2) Maximum number of users that may be connected to a certain femtocell will be lowered, and the burden on the backhaul of femtocell network is decreased.

For the example scenario in Fig. 4.1(b), assuming equal bandwidth per femtocell user after the mMS hand-off to the femtocell, the capacity of the fMS and mMS users with open access can be respectively written as

$$C_{\mathrm{m},i}^{\mathrm{OA}} = \frac{B_{\mathrm{f}}}{F+1} \log \left(1 + \frac{P_{\mathrm{f},i}}{\tilde{I}_{\mathrm{m}} + N_0(B_{\mathrm{f}}/(F+1))} \right) , \tag{4.8}$$

$$C_{\mathrm{f},j}^{\mathrm{OA}} = \frac{B_{\mathrm{f}}}{F+1} \log \left(1 + \frac{P_{\mathrm{f},j}}{\tilde{I}_{\mathrm{m}} + N_0(B_{\mathrm{f}}/(F+1))} \right) , \tag{4.9}$$

[1]Note that while will not be specifically discussed here, averaging of the received signals and multiple threshold tests may further be formulated to avoid the so-called *ping-pong* effects, where the MS may frequently switch links between different cells.

where $i \neq j$ and $\tilde{I}_{\mathrm{m}} < I_{\mathrm{m}}$ due to the i^{th} mMS hand-off to the femtocell. Comparing (4.8) and (4.9) with (4.4) and (4.5), the capacity of the fMS degrades due to reduction of its usable bandwidth, while the capacity of the mMS improves. Since the overall capacity of the MSs and number of fMSs per femtocell are balanced through this approach, we refer it as open access with load balancing (OA-LB). Note that number of users served by the femtocells (or, available bandwidth at the femtocells) needs to be shared between the femtocells and the macrocell in order to implement OA-LB, which, for example, can be communicated through the backhaul connection.

4.3 Simulation Results

4.3.1 Comparison of Dedicated Channel vs. Co-channel Modes

In order to evaluate several trade-offs discussed in previous sections simulations are made. Simulation parameters are selected based mostly on [8] and key set of parameters are summarized in Table 2.3. The downlink of a macrocell/femtocell scenario as in Fig. 2.3 and Fig. 2.4 are considered.

Fig. 4.3 compares the capacities of indoor users for the following cases: with no active femtocells, with femtocells operating in dedicated channel mode, and with femtocells operating in co-channel mode. All results are obtained for wall loss (WL) of 10 dB and 20 dB. The introduction of femtocells, for both channel modes, presents a significant increase in the capacity of indoor users. With a higher signal strength and more bandwidth, this increase in capacity is not surprising. A major factor impacting the performance of femtocell is the level of interference received from the macrocell (in case of co-channel mode) and from neighboring femtocells (in both cases). Another important factor is the available bandwidth for femtocell users, which depends on the number of users served by the femtocell and, for dedicated channel mode, on the allocated portion of the spectrum. In this simulation, 10% of the spectrum allocated to femtocell operating in dedicated mode, and the results in Fig. 4.3 show a clear advantage to co-channel mode over dedicated channel mode for indoor users.

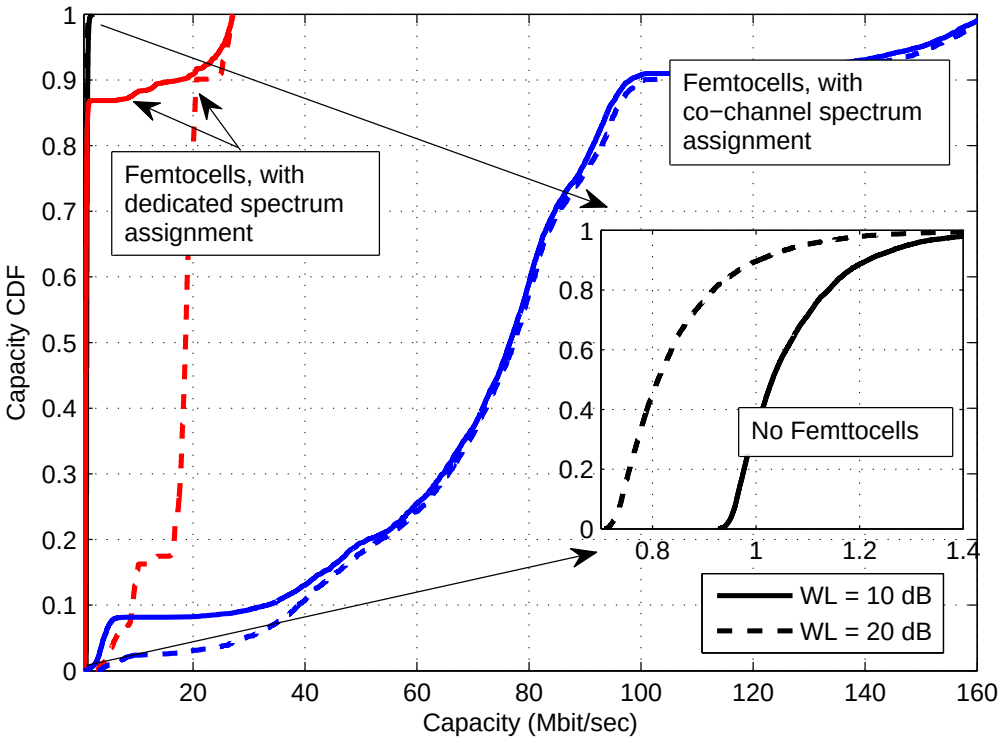

Figure 4.3 Capacity CDFs for no femtocells, dedicated channel femtocells, and co-channel femtocells (indoor users).

Note that in Fig. 4.3, increase in the wall penetration loss reduces the RSS from the mBS. This results in a degradation in the capacity when no femtocells are present. On the other hand, femtocell performance benefits from higher wall penetration loss as it reduces the interference from other fBSs and the mBS, and provides a better isolation for the indoor femtocell. Also, a staircase type of behavior is observed in the capacity CDF of dedicated channel assignment with WL = 10 dB. Reason for this is that for several indoor users closer to the mBS, RSS from the mBS may still be stronger than the RSS from the fBS for smaller WL. Therefore, with SINR based metric, despite the scarcer spectrum resources at the mBS, some MSs may still prefer to connect to the mBS even when they are located indoors. This results in lower capacities for these MSs and deactivation of femtocells that do not have any remaining users.

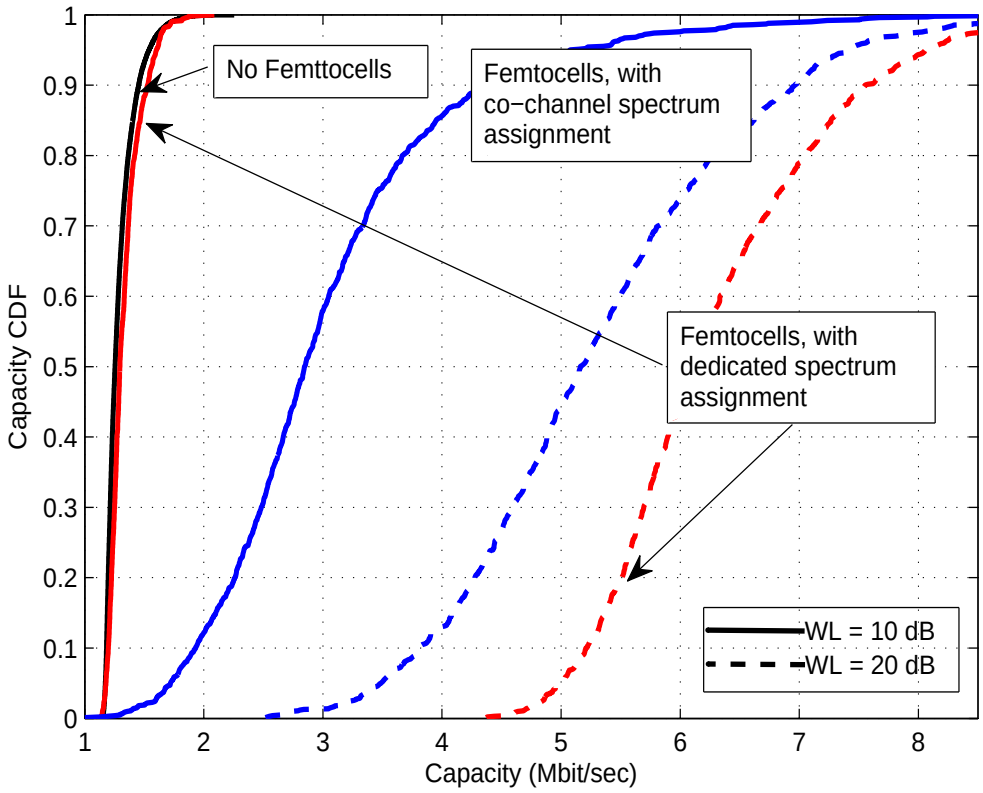

Figure 4.4 Capacity CDFs for no femtocells, dedicated channel femtocells, and co-channel femtocells (outdoor users).

Fig. 4.4 compares the capacities of outdoor users for the same cases considered in the previous figure. Contrary to the case of indoor users, this figure shows that dedicated channel mode outperforms co-channel mode for outdoor users with WL = 20 dB. For the case where WL = 10 dB, RSS of the signal coming from mBS is strong enough to much more indoor users register to mBS which results in less capacity (almost same capacity the one with no femtocells are present) compared to the case where WL = 20 dB. Superiority of dedicated spectrum usage to co-channel spectrum usage with WL = 20 dB comes as a direct result of the separation of operating bands of femtocells and the macrocell which reduces interference caused to outdoor users (who are mainly communicating with the macrocell) from femtocells. However, interference is present in femtocells operating in co-channel mode, causing a decrease in outdoor users capacity. In both cases, the increase in outdoor

Table 4.1 Comparison of median capacities (in Mbps) with and without femtocells.

Users	WL (dB)	No Femto	w/Femto (dc)	w/Femto (cc)
All	20	1.14	15.76	65.42
Indoor	20	0.85	17.27	74.63
Outdoor	20	1.29	5.81	5.27
All	10	1.21	3.19	63.29
Indoor	10	1.07	3.50	72.03
Outdoor	10	1.29	1.30	2.87

users' capacity is caused by the extra bandwidth available to macrocell users as a result of indoor users handing off to femtocells. For higher wall penetration loss, this gain outweighs the loss caused by interference in co-channel mode. Hence, an increase is noticed in the capacity with WL = 20 dB over WL = 10 dB. With dedicated channel mode, the higher wall penetration loss allows more indoor users to hand-off to femtocells leaving more available bandwidth to the macrocell users. This explains the gain in outdoor users capacity with higher penetration loss in dedicated channel mode although they are not under interference from near-by femtocells.

The median capacities of the results in Figs. 4.3-4.4 are summarized in Table 4.1, which confirm that 1) capacity of indoor users may be improved significantly through deploying femtocells, especially for larger WL and for co-channel deployments, and 2) capacity of outdoor users may also be improved due to off-loading effect, especially with dedicated channel deployments.

4.3.2 Open Access with Load Balancing (OA-LB)

For the open access simulations, we consider a scenario as in Fig. 4.5, where there are two fBSs located at $(0, 0)$ m and $(20, 0)$ m, serving to $N_{\text{f1}} = 6$ and $N_{\text{f2}} = 3$ femtocell users, respectively, both having a wall penetration loss of 5 dB. An mBS (not shown on the figure) is located at $(d_{\text{mBS}}/\sqrt{2}, d_{\text{mBS}}/\sqrt{2})$, where d_{mBS} denotes the distance between fBS-1 and the mBS. It is assumed that a total of 10 MHz of spectrum is available, which is used simultaneously by the femtocells and the macrocell (macrocell itself is assumed to be

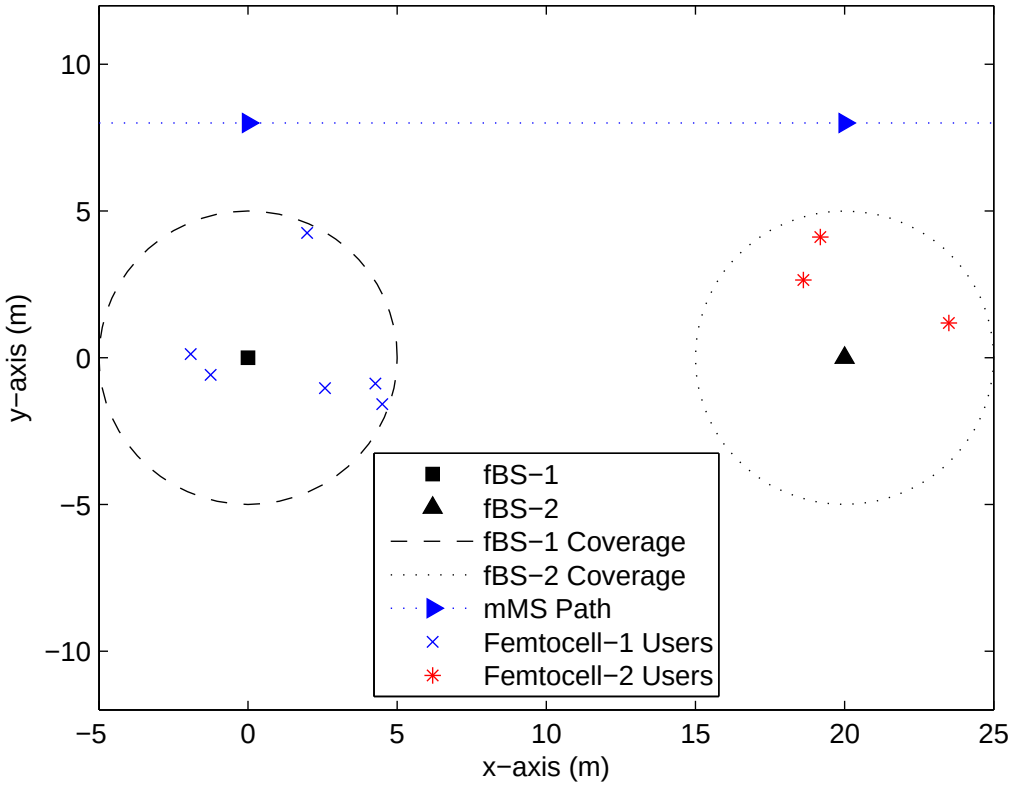

Figure 4.5 Scenario for the open-access simulations.

serving to 100 users). The mMS locations on a line in parallel to the x-axis are considered, from the coordinate $(-40, 8)$ m to $(60, 8)$ m.

Figs. 4.7-4.9 illustrate the capacity of the mMS at different locations and for different d_{mBS}. Best-capacity and best-RSS metrics are both considered for cell selection, and closed access (closed subscriber group (CSG)) results are also included for comparison. When the mBS is closer to the femtocells as in Fig. 4.7, the CSG capacity of the mMS improves due to better signal quality. On the other hand, there is only minimal gain with capacity-maximizing cell selection due to stronger interference from the macrocell to the femtocell. Still, Fig. 4.7 shows that even if the signal quality from the mBS is better, the mMS may achieve better capacities by switching off to Femtocell-2 at certain locations.

Results in Fig. 4.8 and Fig. 4.9 show that as the distance between the mBS and the femtocell increases, capacity maximizing cell selection yields better capacities compared

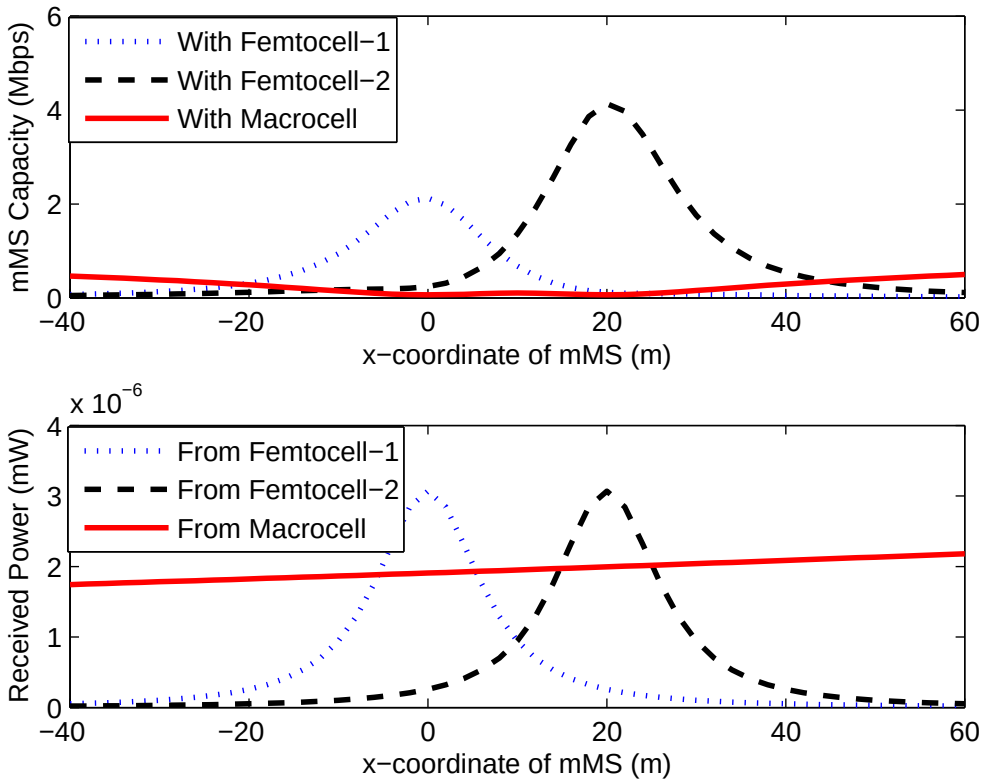

Figure 4.6 Capacity and RSS of mMS for associations with different cells ($d_{\text{mBS}} = 800$ m).

to RSS based cell selection. For $d_{\text{mBS}} = 500$ m, the mMS capacity becomes significantly better when using (4.7) compared to the RSS based cell-selection, especially when the mMS is in the vicinity of the femtocells. For $N_{\text{f2}} = 1$, the mMS capacity improves even further, especially when it is closer to fBS-2. When the mBS distance is further increased to $d_{\text{mBS}} = 800$ m, the RSS from the mBS becomes weaker, and hence the RSS-based and capacity-based metrics give similar results when the mMS is very close to the femtocells. However, it is still possible to obtain better capacities with capacity-maximizing cell selection for certain regions in the vicinity of the femtocells. In all scenarios, both open-access approaches result in better capacities for the mMS compared to the closed access when the mMS is in the vicinity of femtocells.

Fig. 4.10 shows the mean capacity of mMS over the trajectory in Fig. 4.5, for different d_{mBS} and N_{f2} values. The mean CSG capacity degrades in general since the RSS becomes

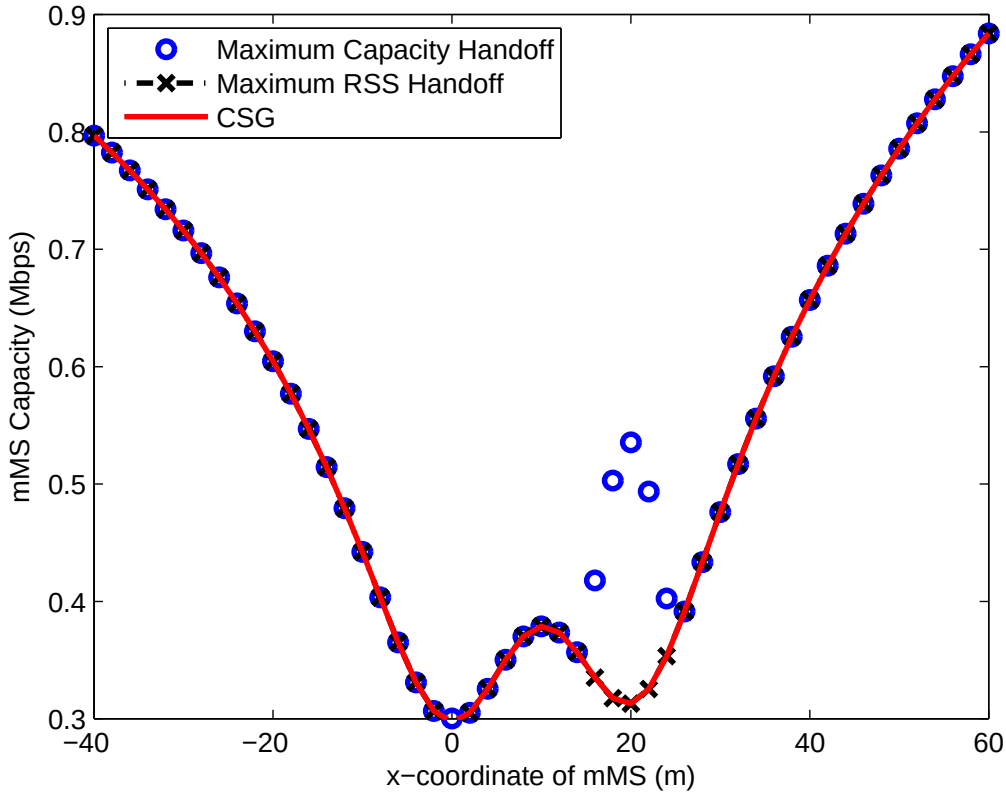

Figure 4.7 Capacity of mMS for different hand-off approaches ($d_{\mathrm{mBS}} = 300$ m.).

weaker for larger d_{mBS}. For very small d_{mBS}, all approaches perform similarly; however, as d_{mBS} increases, capacity-based hand-off starts performing significantly better than other approaches, especially for smaller N_{f2}. For open access methods it is observed that there is a certain d_{mBS} value where the capacity gets minimized.

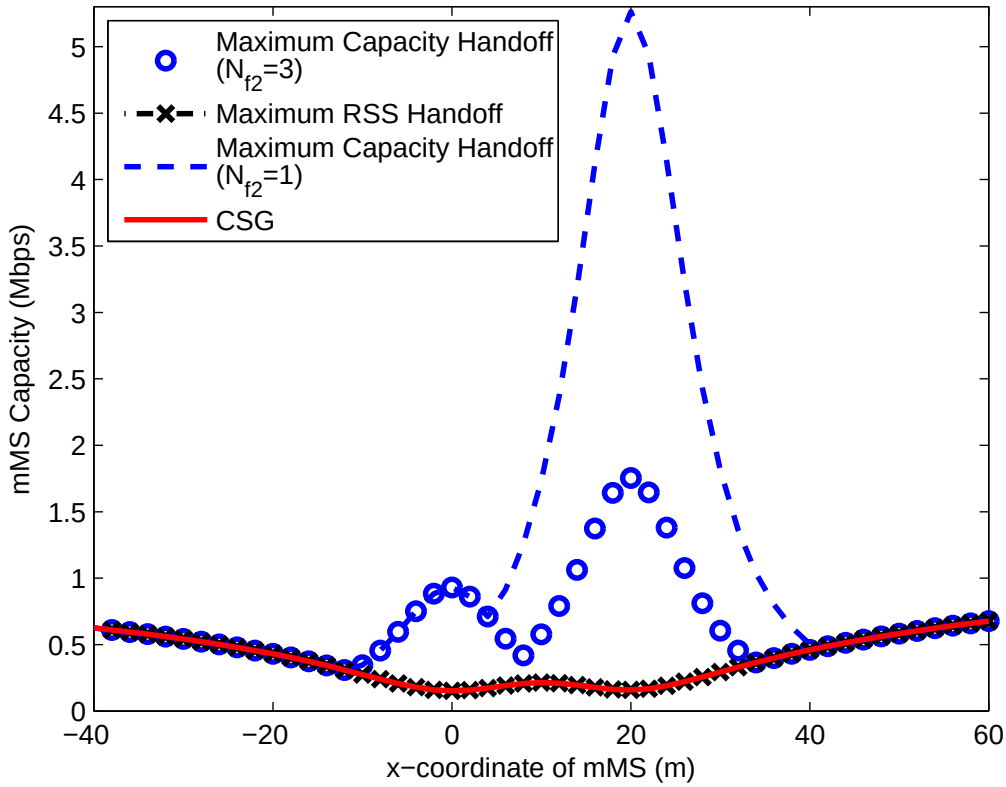

Figure 4.8 Capacity of mMS for different hand-off approaches ($d_{\mathrm{mBS}} = 500$ m.).

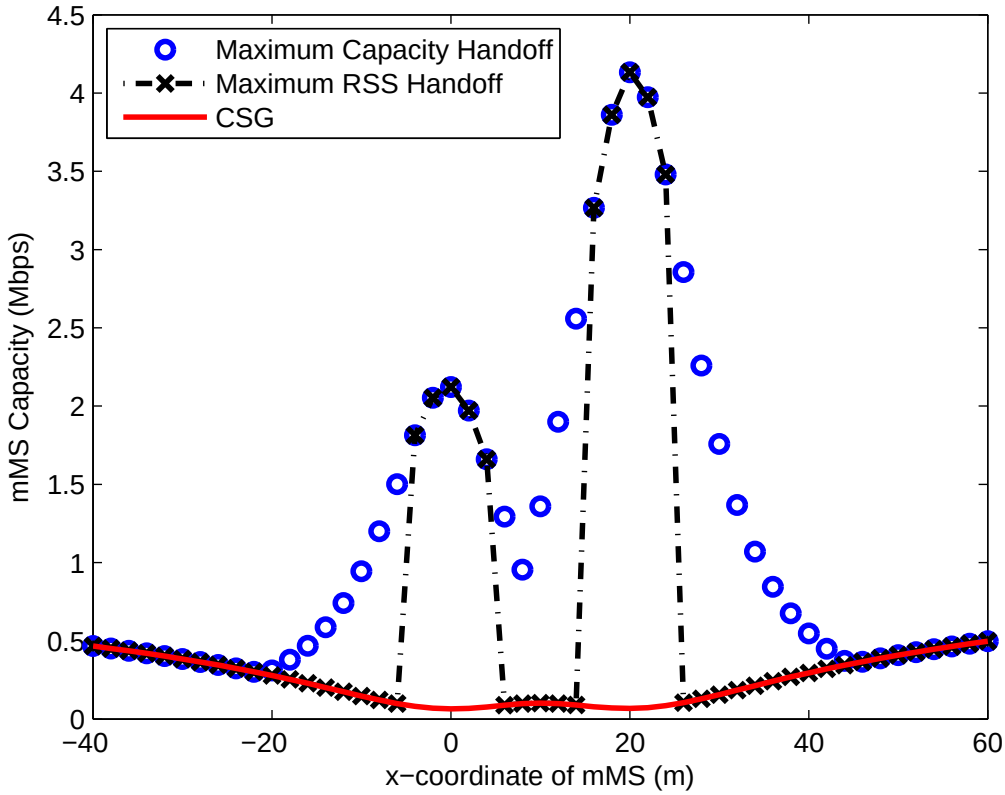

Figure 4.9 Capacity of mMS for different hand-off approaches ($d_{\mathrm{mBS}} = 800$ m.).

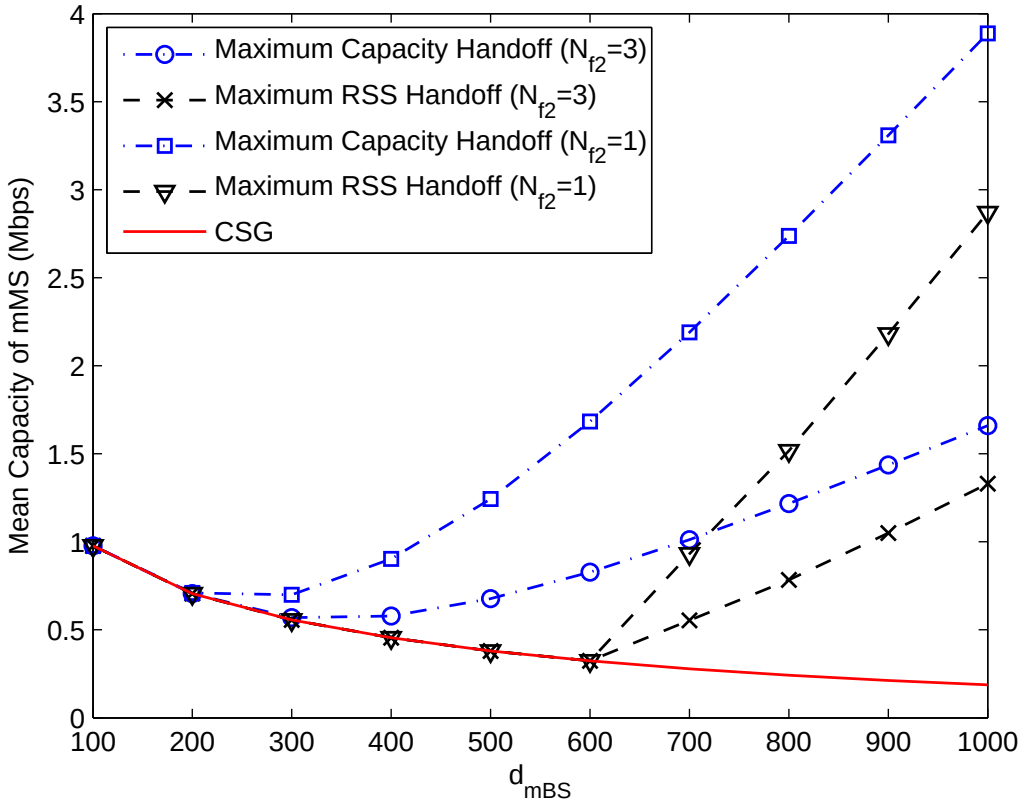

Figure 4.10 Mean capacity of mMS over the trajectory in Fig. 4.5.

CHAPTER 5

CONCLUSION AND FUTURE WORK

Femtocells are designed to change the construction method of mobile operators' cellular networks and improve their coverage and capacity. Femtocells are small and cheap, transmit at such short range, and operate in the licensed cellular bands. They are aimed to be positioned in personal homes and backhauled onto operator's network using conventional DSL and cable broadband access.

Three different techniques are proposed in Chapter 3 for improving the capacity of closed access types of femtocells. The gains are analyzed through Shannon capacity formulations and computer simulations. For the closed access femtocells, capacity improvement is achieved through not using the OB at a femtocell under certain circumstances. Also Chapter 3 includes evaluation of both of the proposed techniques in system-level simulations, and considering realistic spectrum sensing methods for assessing the practicality of the proposed DSR approach.

In Chapter 4, performance improvements through dedicated channel and co-channel femtocell deployments are studied through the help of channel capacity formulations and computer simulations. It is shown that while co-channel operation is preferable from the perspective of indoor users, dedicated channel operation is preferable for causing less interference to outdoor users. Furthermore, deployment of femtocells improves the capacity of not only indoor users, but also outdoor users due to off-loading effect, especially for dedicated channel deployments with larger wall penetration loss. Moreover, a load balancing method is proposed, where a capacity-based metric is used for cell-selection rather than a link-quality based metric; this allows more fair sharing of the spectrum resources among the

macrocell and femtocell users, and lowers the backhaul burden by reducing the maximum number of users in a certain femtocell.

Future work includes the improvements in the simulation tool according to parameters given in Chapter 2 such as introducing the log-normal shadowing to the both macrocell and femtocell channel settings, implementing the sectorization such that every macrocell has three sectors with universal frequency reuse, and introducing the interferences from other macrocells. LTE signal generation, transmission/reception of the generated signal, and obtaining the bit error (BER) curves based on the received signal are also planning as future work. Moreover, theoretical optimization of the proposed methods in Chapter 3 (e.g., optimization of IoT and MML thresholds) for various scenarios is considered as future work.

REFERENCES

[1] F. Chiussi, D. Logothetis, I. Widjaja, and D. Kataria, "Femtocells [Guest Editorial]," *IEEE Communications Magazine*, vol. 48, no. 1, pp. 24–25, 2010.

[2] V. Chandrasekhar, J. G. Andrews, and A. Gatherer, "Femtocell networks: a survey," *IEEE Commun. Mag.*, vol. 46, no. 9, pp. 59–67, Sep. 2008.

[3] F. Chiussi, D. Logothetis, I. Widjaja, and D. Kataria, "Femtocells [Guest Editorial]," *IEEE Communications Magazine*, vol. 47, no. 1, pp. 66–67, 2009.

[4] Airvana, "Femto cells: Personal base stations," 2007, white Paper. [Online]. Available: http://www.airvana.com/files/Femto_Overview_Whitepaper_FINAL_12-July-07.pdf

[5] I. T. . Media, "Femtocell market status," Feb. 2010, white Paper.

[6] "Simulation Assumptions and Parameters for FDD HeNB RF Requirements," 3GPP, 3GPP TGS RAN R4-092042, May 2009.

[7] NTT DOCOMO, "Tp for tr36.814 on heterogeneous network," 3GPP TSG RAN WG1 Meeting R1-101278, San Francisco, USA, pp. 1–5, Feb. 2010.

[8] FemtoForum, "Interference management in UMTS femtocells," White Paper, Dec. 2008. [Online]. Available: http://www.femtoforum.org/femto/Files/File/InterferenceManagementinUMTSFemtocells.pdf

[9] I. Demirdogen, I. Guvenc, and H. Arslan, "Capacity of closed-access femtocell networks with dynamic spectrum reuse," in *submitted to Proc. IEEE Int. Symp. Personal, Indoor, Mobile Radio Commun. (PIMRC)*, Istanbul, Turkey, Sep. 2010, pp. 1–6.

[10] "3rd Generation Partnership Project; Technical Specification Group Radio Access Networks; 3G Home NodeB Study Item Technical Report (Release 8)," 3GPP, 3GPP TR 25.820, March 2008.

[11] S. P. Yeh, S. Talwar, S. C. Lee, and H. Kim, "WiMAX femtocells: a perspective on network architecture, capacity, and coverage," *IEEE Commun. Mag.*, vol. 46, no. 10, pp. 58–65, Oct. 2008.

[12] D. L. Perez, A. Valcarce, G. D. L. Roche, E. Liu, and J. Zhang;, "Access methods to WiMAX femtocells: A downlink system-level case study," in *Proc. IEEE Int. Conf. Commun. Syst. (ICCS)*, Guangzhou, China, Nov. 2008, pp. 1657–1662.

[13] H. Claussen, "Performance of macro- and co-channel femtocells in a hierarchical cell structure," in *Proc. IEEE Int. Symp. Personal, Indoor, Mobile Radio Commun. (PIMRC)*, Athens, Greece, Sep. 2007, pp. 1–5.

[14] NTT DOCOMO, " Downlink Interference Coordination Between eNodeB and Home eNodeB," 3GPP TSG RAN WG1 Meeting R1-101225, San Francisco, USA, pp. 1–8, Feb. 2010.

[15] Y. Bai, J. Zhou, and L. Chen, "Hybrid spectrum sharing for coexistence of macrocell and femtocell," in *IEEE International Conference on Communications Technology and Applications*, Beijing, Oct. 2009, pp. 1–5.

[16] Y.-Y. Li, M. Macuha, E. S. Sousa, T. Sato, and M. Nanri, "Cognitive interference management in 3g femtocells," in *Proc. IEEE Int. Symp. Personal, Indoor, Mobile Radio Commun. (PIMRC)*, Tokyo, Japan, Sep. 2009, pp. 1–5.

[17] NTT DOCOMO, "Views on Deployment Scenarios in Heterogeneous Networks," 3GPP TSG RAN WG1 Meeting R1-094916, Tokyo, Japan, pp. 1–4, Nov. 2009.

[18] "Guidelines for evaluation of radio interface technologies for imt-advanced," ITU-R Report M.2135, Nov. 2008.

[19] "3rd Generation Partnership Project; Technical Specification Group Radio Access Networks; Further Advancements for E-UTRA Physical Layer Aspects(Release 9)," 3GPP, 3GPP TR 36.814, Nov. 2009.

[20] "Considerations on Interference Coordination in Het-Net," 3GPP TSG RAN WG1 Meeting R1-100902, San Francisco, USA, Feb. 2010.

[21] S. Sesia, I. Toufik, and M. Baker, *LTE, The UMTS Long Term Evolution: From Theory to Practice*. Wiley Publishing, 2009.

[22] M. Yavuz, F. Meshkati, S. Nanda, A. Pokhariyal, N. Johnson, B. Raghothaman, and A. Richardson, "Interference management and performance analysis of UMTS/HSPA+ femtocells-[femtocell wireless communications]," *IEEE Communications Magazine*, vol. 47, no. 9, pp. 102–109, 2009.

[23] D. López-Pérez, A. Valcarce, G. De La Roche, J. Zhang, *et al.*, "OFDMA femtocells: a roadmap on interference avoidance," *IEEE Communications Magazine*, vol. 47, no. 9, pp. 41–48, 2009.

[24] I. Guvenc, M. R. Jeong, F. Watanabe, and H. Inamura, "A hybrid frequency assignment for femtocells and coverage area analysis for co-channel operation," *IEEE Commun. Lett.*, vol. 12, no. 12, pp. 880–882, Dec. 2008.

[25] V. Chandrasekhar and J. G. Andrews, "Uplink capacity and interference avoidance for two-tier cellular networks," in *Proc. IEEE Global Telecommun. Conf. (GLOBECOM)*, Washington, DC, Nov. 2007, pp. 3322–3326.

[26] K. Y. Lin, H. P. Lin, and R. T. Juang, "Proposed text for HO from femtocell BS to macro BS or other femtocell BS (AWD-femto)," IEEE Standard Contribution C802.16m-09/1307, July 2009.

[27] I. Demirdogen, I. Guvenc, and H. Arslan, "Capacity analysis of open-access femtocell networks," in *submitted to Proc. IEEE Int. Symp. Personal, Indoor, Mobile Radio Commun. (PIMRC) Workshop*, Istanbul, Turkey, Sep. 2010.